JOURNAL OF GEOPHYSICAL RESEARCH, VOL. 103, NO. D1, PAGES 1527-1547, JANUARY 20, 1998

The effects of sulfur emissions from HSCT aircraft: A 2-D model intercomparison

Debra K. Weisenstein,[1] Malcolm K. W. Ko,[1] Igor G. Dyominov,[2] Giovanni Pitari,[3] Lucrezia Ricciardulli,[3,5] Guido Visconti,[3] and Slimane Bekki[4,6]

Abstract. Four independently formulated two-dimensional chemical transport models with sulfate aerosol microphysics are used to evaluate the possible effects of sulfur emissions from high-speed civil transport (HSCT) aircraft operating in the stratosphere in 2015. Emission scenarios studied are those from *Baughcum and Henderson* [1995], while assumptions regarding the form of emitted sulfur are similar to those of *Weisenstein et al.* [1996]. All models show much larger increases in aerosol surface area when aircraft sulfur is assumed to be emitted as particles of 10 nm radius rather than as gas phase SO_2. If we assume an emission index (EI) for SO_2 of 0.4 gm (kg fuel burned)$^{-1}$ in 2015, maximum increases in stratospheric sulfate aerosol surface area range from 0.1 μm^2 cm^{-3} to 0.5 μm^2 cm^{-3} with sulfur emitted as SO_2 gas and from 1.0 μm^2 cm^{-3} to 2.5 μm^2 cm^{-3} with sulfur emitted as particles. Model differences in calculated surface area are deemed to be due mainly to differences in model transport. Calculated annual average ozone perturbations due to aircraft emissions with EI(NO_x)=5, EI(H_2O)=1230, and EI(SO_2)=0.4 range from -0.1% to -0.6% at 45°N for sulfur emission as SO_2 gas and from -0.4% to -1.5% with sulfur emission as 100% particles. The effect of zonal and temporal inhomogeneities in temperature on heterogeneous reactions rates is accounted for in the Atmospheric and Environmental Research model and the Università degli Studi L'Aquila model and significantly increases the calculated ozone depletion due to HSCT, particularly for the cases with concurrent increases in aerosol surface area. Sensitivities to polar stratospheric clouds, background chlorine amount, additional heterogeneous reactions, and background aerosol loading are also explored.

1. Introduction

High-speed civil transport aircraft, known as HSCTs, could be flying commercial routes by 2015. These aircraft would operate at cruise speeds between Mach 2.0 and Mach 2.4, which necessitate flying in the stratosphere at altitudes between 18 and 21 km. HSCT engines are expected to emit large amounts of water vapor and carbon dioxide and relatively small amounts of nitrogen oxides (NO_x), sulfur dioxide, carbon monoxide, and hydrocarbons. These emissions could perturb stratospheric chemistry, aerosol concentrations, and ozone. Early studies [e.g., *Johnston et al.*, 1989] indicated that NO_x emissions have the largest effect on ozone, leading to significant decreases. Formal assessments of the effects of HSCTs have been performed under the NASA Atmospheric Effects of Aviation Program (AEAP), which has reported predicted changes in ozone from a number of two-dimensional (2-D) atmospheric models, based on forecast emission scenarios of a global fleet of 500 HSCT aircraft [*Albritton et al.*, 1993; *Stolarski et al.*, 1995]. These more recent assessments have included the effects of heterogeneous chemistry occurring on the background sulfate aerosol layer [*World Meteorological Organization (WMO)*, 1993], which has been found to significantly decrease ozone sensitivity to HSCT NO_x emissions [*Weisenstein et al.*, 1991; *Bekki et al.*, 1991]. However, they have not considered possible perturbations to the sulfate aerosol layer by emission of sulfur from HSCT engines.

Some 2-D studies of the effect of HSCT sulfur emissions have been conducted by individual modeling groups. *Bekki and Pyle* [1993] modeled the impact of a fleet of HSCTs, assuming an emission index (EI) for NO_x of 20 (i.e., 20 g NO_2 per kilogram of fuel burned)

[1]Atmospheric and Environmental Research, Inc., Cambridge, Massachusetts.
[2]Department for Atmospheric Research, Novosibirsk State University, Novosibirsk, Russia.
[3]Dipartimento di Fisica, Università degli Studi L'Aquila, L'Aquila, Italy.
[4]Center for Atmospheric Science, Department of Chemistry, University of Cambridge, England.
[5]Now at National Center for Atmospheric Research, Boulder, Colorado.
[6]Permanently at Service d'Aeronomie du CNRS, Institut Pierre-Simon Laplace, Universite Paris, Paris, France.

Paper number 97JD02930.
0148-0227/98/97JD-02930$09.00

and EI(SO_2) of 2 (i.e., 2 g SO_2 per kilogram of fuel burned). They concluded that the SO_2 emissions could potentially double the aerosol surface area of the northern hemisphere lower stratosphere. *Bekki and Pyle* [1993] found decreased sensitivity of ozone to HSCT emissions for their model scenario but pointed out that the increased aerosol levels also increased the model sensitivity to chlorine abundance in the lower stratosphere. *Pitari et al.* [1993] modeled an emission scenario with EI(NO_x)=15 and EI(SO_2)=1.0. They found increases in aerosol surface area in the northern hemisphere lower stratosphere of up to 60% along with enhanced ozone depletion. *Tie et al.* [1994] also used EI(NO_x)=15 and EI(SO_2)=1.0. They predicted a 10-20% increase in aerosol surface area and found that the associated ozone changes were small in comparison with the total impact of HSCT emissions. The above studies were performed by putting the sulfur emissions along the flight paths as gas phase SO_2. *Weisenstein et al.* [1996] modeled an HSCT scenario with EI(NO_x)=5 and EI(SO_2)=0.4, evaluating the impact with sulfur emissions assumed to be all gas phase SO_2, all 10 nm particles, and a 10% particles/90% SO_2 gas mix. Increases in sulfate aerosol surface area were found to be up to 50% for sulfur emission as SO_2 gas and up to 200% when emissions were assumed to be all particles. Ozone depletion due to HSCTs was enhanced by the increased sulfate surface area, from 0.1% without sulfur emissions to 1.3% with sulfur emissions as 100% particles with 3 ppbv of chlorine on an annual average basis at 47°N.

Because the previously discussed modeling results used different emission scenarios and contained variations in chemical reaction rates and background gas concentrations, the results cannot be compared directly. This paper will present results from four independently formulated 2-D stratospheric models, each of which includes sulfate aerosol microphysics and uses identical emission scenarios and standardized chemical rates [from *DeMore et al.*, 1994]. These models are the Atmospheric and Environmental Research (United States) 2-D model, the University of Cambridge (England) 2-D model, the Università degli Studi L'Aquila (Italy) 2-D model, and the Novosibirsk State University (Russia) 2-D model. While these models can calculate aerosol microphysics on the scale of their model grid boxes (typically 10° latitude by 2 km in the vertical), they cannot account for microphysics and heterogeneous chemical processing that may occur in the aircraft plume or wake. Conditions in the wake, particularly in the first few seconds after emission, are very different from ambient conditions. Sulfur dioxide may be converted to SO_3 or H_2SO_4 in the early stages of wake evolution or in the engine or nozzle [*Brown et al.*, 1996b]. As a result of the high supersaturations possible in an aircraft wake, H_2SO_4 can form new sub-micron size aerosol particles through homogeneous nucleation or by condensation onto soot particles [*Brown et al.*, 1996c; *Kärcher and Fahey*, 1997]. A very high density of aerosol particles would lead to substantial coagulation in the wake [*Kärcher and Fahey*, 1997; *Danilin et al.*, 1997]. The detailed chemistry and physics of sulfur in aircraft plumes are not well known. Nevertheless, a recent stratospheric measurement in the plume of the Concorde aircraft [*Fahey et al.*, 1995] indicated that a substantial fraction of the emitted sulfur was converted to aerosol particles within 16 min after exhaust. A measurement of aerosols in the exhaust trail of a military aircraft at 23 km [*Hofmann and Rosen*, 1978] indicated nearly complete conversion of emitted sulfur to aerosols after 18 hours.

The 2-D models employed in this study will adopt assumptions regarding the atmospheric state of the emitted sulfur at the point when the emitted material is diluted to grid box size (a time period of roughly 1 week). This approach will enable us to calculate the global impact of aircraft sulfur emissions in lieu of knowing the details of chemistry in the engine, nozzle, and wake regimes. The amount of sulfur put into each grid box is given by the product of the adopted EI for SO_2 and the fuel burn in that grid box. We consider three assumptions regarding the phase of the emitted sulfur: (1) all sulfur remains in the form of SO_2 gas, (2) 10% of the emitted sulfur is converted to aerosol particles of 10 nm radius, and (3) 100% of the emitted sulfur is converted to 10 nm aerosol particles. Greater changes in the aerosol surface area of the stratosphere are to be expected under assumption 3. The 100% conversion of aircraft-emitted sulfur to aerosol particles within 1 week cannot be ruled out on the basis of atmospheric measurements to date, so we take this case as the upper limit. Assumption 2 represents the lower limit of aerosol formation in the plume as determined by the Concorde measurements [*Fahey et al.*, 1995] within 1 hour of emission. Assumption 1 is included for historical reasons and is similar to theoretical calculations for aerosol formation in aircraft plumes when sulfur is assumed emitted as SO_2 and reaction with OH is the only oxidation mechanism [*Brown et al.*, 1996a].

We will start with descriptions of the four models to be used in this comparison, including the similarities and differences of their microphysical, chemical, and dynamical formulations, in section 2. Section 3 will describe the HSCT scenario used and present results of changes in sulfate surface area and ozone. Section 4 will present additional sensitivity studies that have been performed by subsets of the four models. Section 5 will summarize the results and draw conclusions.

2. Model Descriptions and Comparisons

2.1. Atmospheric and Environmental Research Model

The Atmospheric and Environmental Research (AER) sulfur model is described by *Weisenstein et al.* [1997]. Aerosol processes modeled include homogeneous nucleation, coagulation, condensation/evaporation, and sed-

imentation. There are 40 aerosol size bins ranging from 0.39 nm to 3.2 μm by volume doubling. Only binary sulfuric acid-water aerosols are considered. The sulfur model is not coupled to the ozone model in that the OH field in the sulfur model is fixed at precalculated values. The sulfate surface area density calculated by the sulfur model is treated as input to the photochemical model. The photochemical model with full O_x, HO_x, CHO_x, NO_x, ClO_x, and BrO_x chemistry is described by *Prather and Remsberg* [1993] and *Weisenstein et al.* [1996]. Model temperature and circulation are prescribed according to climatology and do not respond to changes in aerosols or chemical species.

A temperature probability distribution is employed for the calculation of homogeneous nucleation rates and all temperature-dependent reaction rates following the methodology of *Considine et al.* [1994]. Monthly zonal mean temperature statistics in 1 K increments were derived for the time period from 1979 to 1986 on the basis of daily data from the National Centers for Environmental Prediction/National Center for Atmospheric Research reanalysis project [*Kalnay et al.*, 1996]. The tropical pipe circulation [*Plumb*, 1996] is employed as described by *Weisenstein et al.* [1996], using small values of horizontal diffusion in the tropical lower stratosphere. Grid resolution is 9.5° latitude by 1.2 km in the vertical. Updates to the sulfur model [*Weisenstein et al.*, 1997] since the publication of previous HSCT assessment results [*Weisenstein et al.*, 1996] have somewhat reduced the calculated increases in aerosol surface area due to HSCT emissions; however, inclusion of the temperature probability distribution for calculation of reaction rates has increased the calculated ozone depletion for the same scenarios.

2.2. Novosibirsk State University Model

Included here is a fairly detailed description of the Novosibirsk State University (NSU) model, as this model has not previously been described in an English language journal. The NSU model is a zonally averaged 2-D interactive model for self-consistent calculation of diabatic circulation, temperature, and gaseous and aerosol composition of the troposphere and stratosphere. The photochemical and radiative parts of the model are described by *Dyominov* [1988, 1991, 1992], *Dyominov and Zadorozhny* [1989], *Ginzburg and Dyominov* [1989], and Dyominov et al. (unpublished material, 1992). In this work, circulation and temperature are calculated self-consistently with 45 minor gas constituents: O_3, $O(^3P)$, $O(^1D)$, H, OH, HO_2, H_2O_2, H_2O, NO, NO_2, NO_3, N_2O_5, HNO_3, HNO_4, N_2O, CO, CH_4, CH_3, CH_2O, CH_3O_2, CH_3CO, CH_3CO_3, $CH_3CO_3NO_2$ (peroxyacetyl nitrate), Cl, ClO, HOCl, $ClONO_2$, HCl, CCl_4, CH_3Cl, Br, BrO, HOBr, HBr, $BrONO_2$, CH_3SCH_3 (dimethylsulfide, or DMS), CS_2, H_2S, OCS, S, SO, SO_2, SO_3, HSO_3, and H_2SO_4. Additional chlorine and bromine source gases are included in the model but not calculated interactively. These include the organic chlorine species $CFCl_3$ (CFC-11), CF_2Cl_2 (CFC-12), $CF_2ClCFCl_2$ (CFC-113), CHF_2Cl (HCFC-22), CH_3CFCl_2 (HCFC-141b), and CH_3CCl_3 and the organic bromine species CH_3Br, CF_3Br (H-1301) and CF_2ClBr (H-1211), which are calculated only for a background atmosphere representing the year 2015 (3.0 ppbv or 2.0 ppbv of Cl_y and 17 pptv of Br_y).

Interaction of all these gaseous components is governed by 157 photochemical reactions, including 26 reactions that describe interactions among the sulfate components. The diurnal variation of photolysis rates is recalculated every tenth model day. Five heterogeneous reactions are used to account for interactions between gaseous components and aerosol particles (see reactions (1)-(4) in section 2.5 and reaction (5) in section 4.4 below). The rates of heterogeneous reactions (1)-(3) and (5) are calculated by using the formula $k = \gamma V_T S/4$, where γ is the reaction probability, V_T is the thermal velocity of gas molecules, and S is the surface area density of sulfate aerosols. Values of γ for heterogeneous reactions (1)-(3) are taken from Table 3-2 of *WMO* [1993]: γ_1=0.1, $\log_{10}(\gamma_2) = 1.87 - 0.074W$, where W is the weight percent of H_2SO_4 in aerosol particles (calculated according to the formula of *Hanson et al.* [1994]), and $\gamma_3 = 0.1\gamma_2$. The rate of heterogeneous reaction (4) is calculated according to the method of *Hanson et al.* [1994] and is proportional to the volume of the aerosol particles. The constant value 0.4 [*Hanson and Ravishankara*, 1995] is adopted for the probability of heterogeneous reaction (5).

The temperature stratification of the atmosphere is determined by the heat balance equation. Calculation of atmospheric heating and cooling rates takes into account heat fluxes due to convection, turbulent heat exchange, and radiative transfer in three spectral ranges: UV and visible (0.175-0.9 μm), near infrared (0.9-4.0 μm), and infrared (>4.0 μm). The radiative fluxes in the UV and visible part of the spectrum are computed by taking into account scattering on air molecules and aerosol particles, reflection from clouds and the Earth's surface, and absorption by oxygen, ozone, and nitrogen dioxide. In the near infrared, absorption by water vapor (in the 0.94, 1.1, 1.38, 1.87, 2.7, and 3.2 μm bands) and by carbon dioxide (in the 2.0 and 2.7 μm bands) is considered. Infrared fluxes account for longwave radiative absorption by CO_2, O_3, H_2O, CH_4, N_2O, $CFCl_3$, and CF_2Cl_2. The fine spectral structure of these constituents is taken into account in absorption bands centered around 15 μm for CO_2; 9.6 μm for O_3; 6.3 μm for H_2O; 7.6 μm for CH_4; 4.5, 7.78, 8.57, and 17 μm for N_2O; 9.22 and 11.82 μm for $CFCl_3$; and 8.68, 9.13, and 10.93 μm for CF_2Cl_2. For H_2O, rotational bands are also taken into account.

Dynamical processes in the atmosphere are represented in the model by the residual circulation and eddy diffusion. The method of computing the residual circulation is described by *Ginzburg and Dyominov* [1989] and *Talrose et al.* [1993]. It consists of solving the

zonally averaged equations describing conservation of momentum, mass, and energy, with the momentum flux divergence due to gravity waves approximated by means of a Rayleigh friction coefficient [*Garcia and Solomon,* 1983]. The momentum flux due to breaking planetary waves is parameterized as in the model of *Hitchman and Brasseur* [1988]. The eddy diffusion coefficients are computed by using the method described by *Brasseur et al.* [1990]. The model grid resolution is 5° latitude and 1 km in the vertical for altitudes up to 36 km, with 2 km vertical resolution from 36 to 50 km.

The 2-D model of aerosol composition of the troposphere and stratosphere is described by *Golitsyn et al.* [1994]. The results of calculations with this model are also described by *Dyominov and Elansky* [1995], *Dyominov et al.* [1995], and *Dyominov and Zadorozhny* [1996]. The aerosol 2-D model can calculate distributions of three types of aerosol particles: ice, nitric acid trihydrate (NAT), and sulfate particles, though only sulfate particles are treated in the present study. There are 30 aerosol bins in the model, with particle radii ranging from 6.4 nm to 5.2 μm by volume doubling. Microphysical processes simulated are nucleation (both homogeneous and heterogeneous), condensation, evaporation, coagulation, sedimentation, and washout. The classical approach is used for the calculation of the binary homogeneous nucleation rate, as discussed by *Frenkel* [1975] and *Hamill et al.* [1982]. The heterogeneous nucleation rate is calculated according to the method given by *Hamill et al.* [1982] and employed by *Pitari et al.* [1993]. Concentrations of Aitken nuclei (0.012 μm $\leq r \leq$ 0.4 μm) and large nuclei (0.5 μm $\leq r \leq$ 2.0 μm) at a surface of the Earth were assumed equal to 1800 cm^{-3} and 40 cm^{-3}, respectively. Condensation and evaporation are calculated in the model following *Turco et al.* [1979] and *Toon et al.* [1988]. Changes of particle size distribution resulting from Brownian coagulation are described with classical relations, as described by *Asaturov et al.* [1986]. Sedimentation of aerosols and tropospheric washout follow *Pitari et al.* [1993].

2.3. Università degli Studi-L'Aquila (Italy) Model

The Università degli Studi-L'Aquila model (hereafter referred to as the Italy model) is described by *Pitari et al.* [1993]. The sulfate aerosol module calculates particle densities in 11 size bins between 0.01 and 10.25 μm radius by radius doubling. Microphysical processes modeled include heterogeneous nucleation, condensation, evaporation, coagulation, and sedimentation. All aerosols are assumed to contain a solid core. Polar stratospheric cloud (PSC) particle distributions (both NAT and ice) can be calculated by the Italy model but are not included here. The grid resolution is 10° latitude by 2.8 km altitude. The circulation is taken from the group's spectral quasi-geostrophic three-dimensional model [*Pitari et al.,* 1992] but is not interactive in these calculation. Temperatures above 20 mbar are taken from the same three-dimensional model and below 20 mbar from standard references. A temperature distribution is applied at each model grid point by assuming a statistical standard deviation [*Pitari,* 1993]. The temperature distribution is applied to the calculation of the rates of the heterogeneous reactions $ClONO_2$+H_2O, $ClONO_2$+HCl, and HOCl+HCl.

2.4. University of Cambridge Model

The University of Cambridge 2-D model is described by *Bekki and Pyle* [1992, 1993]. It treats aerosol particles in 25 size bins between 0.01 and 2.5 μm with volume doubling bin spacing. Microphysical processes included in the Cambridge model are heterogeneous and homogeneous nucleation, condensation, evaporation, coagulation, and sedimentation. The homogeneous nucleation is parameterized by assuming arbitrarily that new sulfuric acid particles are formed at a constant rate [*Bekki and Pyle,* 1992] in the tropical upper troposphere in order to provide a source of nuclei in this region [*Brock et al.*, 1995]. *Hamill et al.* [1982] tested various nucleation mechanisms and found that a simple nucleation treatment led to overall aerosol properties similar to those obtained with sophisticated schemes. The model includes only DMS and carbonyl sulfide (OCS) as sulfur source gases, ignoring surface emissions of SO_2. n The Cambridge model is a classical Eulerian model. The grid resolution is 9.5° latitude and 3.5 km in the vertical. The temperature and circulation are calculated interactively from forcing terms, which include solar heating by O_2 and O_3 and longwave cooling by CO_2, H_2O, O_3, N_2O, and CH_4. The chemical scheme includes what are thought to be the most important reactions of O_x, NO_y, HO_x, ClO_y, BrO_y, CHO_x, and SO_x. A temperature distribution is employed for the calculation of heterogeneous reaction probabilities. Monthly zonal mean temperature statistics are taken from Cospar International Reference Atmosphere [*Labitzke et al.*, 1985] climatologies. The reaction probabilities are as described for the NSU model, with γ of $ClONO_2$+HCl set to a tenth of the reaction probability of $ClONO_2$+H_2O. The reaction HOCl+HCl is not included.

2.5. Model Similarities and Differences

All four models employ fairly standard classical approaches to aerosol microphysics. The processes of condensation, evaporation, coagulation, and sedimentation are treated similarly in all the models. None of the model simulations presented in this paper include PSC chemistry. While some models use heterogeneous nucleation and some use homogeneous nucleation (the NSU model uses both), nucleation is a minor process in the stratosphere (compared with condensation and coagulation) and probably does not lead to large differences in the model results to be presented here. The models also differ in the resolution and range of aerosol sizes considered. The number of size bins varies from 11 to 40 in the models, with the AER and NSU models including

aerosol radii less than 0.01 μm and the Italy and NSU models including the largest sizes. The AER, Cambridge, and NSU models have the same size resolution, using a volume doubling scheme. The Italy model has a coarser resolution, using a radius doubling scheme. A lower size resolution has been found to produce a shift in the size distribution toward larger particles [*Larsen*, 1991].

The most important differences between the models are not in their microphysical formulations but in their transport circulations, temperature fields, and chemical formulations. The Cambridge and NSU models calculate temperature and circulation interactively, while the Italy model takes these fields from an off-line calculation. The AER model prescribes them (using observed climatological temperatures). Temperature fields partially determine aerosol composition and the vertical extent of the aerosol layer. Results from perturbation studies in 2-D models always contain some dependence on model transport, and there is no "standard" or "best" 2-D climatological transport circulation available. Thus each modeling group uses a set of winds and eddy diffusion coefficients that each has found to provide calculated values of ozone and other trace gases that compare favorably with observations. The combination of transport rates and diffusion coefficients that meet these criteria is not unique, and each set leads to somewhat different results in perturbation studies. Indeed, the model comparison presented by *WMO* [1995] indicates intermodel differences of up to 0.7 ppbv in Cl_y concentrations at 50°N and 22 km despite identical boundary conditions.

The method of obtaining diurnal averages of concentrations of short-lived radical species differs between the models and probably accounts for some of the differences in sensitivity of ozone to NO_x, ClO_x, and HO_x concentrations. Though chemical rate coefficients are taken from JPL-94 [*DeMore et al.*, 1994] in all four models, the model calculated OH concentrations are different, and therefore rates of conversion from SO_2 to H_2SO_4 are different. The models include heterogeneous reactions on sulfate aerosols, namely,

$$N_2O_5 + H_2O \rightarrow 2HNO_3 \quad (1)$$

$$ClONO_2 + H_2O \rightarrow HNO_3 + HOCl \quad (2)$$

$$ClONO_2 + HCl \rightarrow HNO_3 + Cl_2 \quad (3)$$

$$HOCl + HCl \rightarrow H_2O + Cl_2 \quad (4)$$

of which reaction (1) is the most important on a global basis. Reactions (2)-(4) are important in the cold regions at high latitudes in winter and under high aerosol conditions. The importance of reactions on cold sulfate aerosol has been demonstrated in analysis of the observed partitioning of the radicals in both satellite and aircraft data [*Michelsen et al.*, 1997]. The use of a temperature probability distribution in the AER and Italy models leads to enhanced importance of these reactions due to their strong temperature dependence. Rates for reactions (2)-(4) in the AER and Italy models are taken from *Hanson et al.* [1994], while all models use a constant γ of 0.1 for reaction (1).

3. Model Intercomparison

The sulfate aerosol surface area calculated by each of the models for annual average background (nonvolcanic) conditions is shown in Figure 1. That derived from Stratospheric Aerosol and Gas Experiment (SAGE) data and adopted by modelers to represent clean background conditions [*WMO*, 1993] is shown in Figure 1f, and the April 1991 surface area [*Yue et al.*, 1994] derived from SAGE II is shown in Figure 1e. The first half of 1991 (before the Mount Pinatubo eruption in June) represents a recent year that is near background conditions, though it probably includes some residual effects of volcanic activity [*Thomason et al.*, 1997]. The actual distribution of aerosol surface area during background conditions is not well known and would of course vary from year to year.

All models reproduce the magnitude and structure of the WMO surface area, with lowest values in the tropical lower stratosphere and highest values in the high latitude lower stratosphere. In comparison with WMO the aerosol surface area of the Cambridge model is 30% low in the tropical lower stratosphere, while the Italy model is 30% high in this region. The NSU model matches WMO most closely. The AER and NSU models predict greater surface area in the northern polar region, on an annual average basis, than in the southern polar region, while the Italy model and WMO show greater surface area in the southern polar region. The Cambridge model is relatively symmetrical between hemispheres. Model tropospheres vary considerably depending on the surface sources of sulfur included in the models. The Cambridge model includes only DMS and OCS surface sources, while other models also include CS_2, H_2S, and SO_2 surface emissions. Surface emissions of SO_2 are evenly distributed with latitude in the Italy and NSU models but are weighted toward the northern hemisphere in the AER model.

Each model was run with identical parameters for aircraft emissions and similar background atmospheres, with a chlorine content of 3.0 ppbv and bromine content of 17 parts per trillion by volume (pptv). The aircraft emission scenarios employed here are those described by *Stolarski et al.* [1995]. These represent 500 aircraft operating in the year 2015 and burning 82×10^9 kg of fuel annually, with the geographical fuel use distribution derived by *Baughcum and Henderson* [1995]. The HSCT aircraft cruise at Mach 2.4, with a cruise altitude of 18-21 km. Engine emissions are specified by an emission index, or EI, defined as grams of pollutant emitted per kilogram of fuel burned. We present results for two values of EI(NO_x), 5 and 15. An EI(NO_x) of 5 represents a significant reduction in emission index from current supersonic aircraft (values of about 20 are typical), though technological advances in the last several

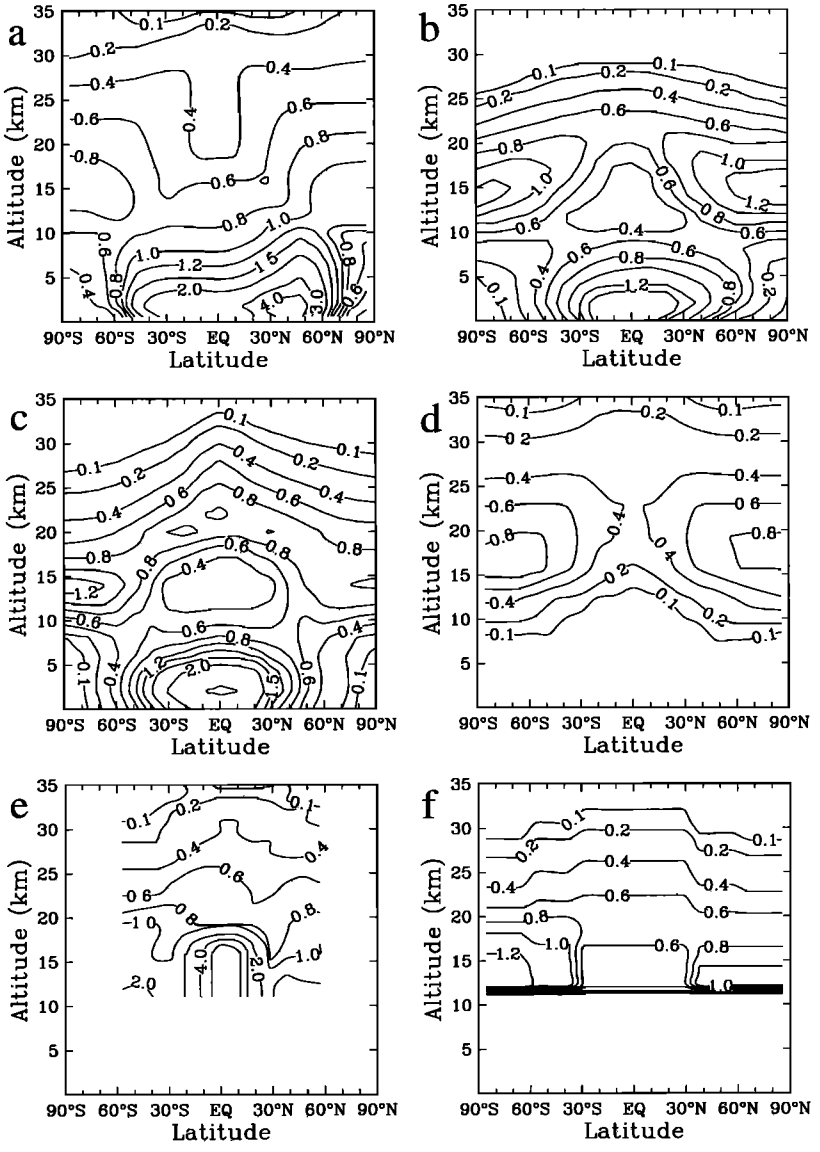

Figure 1. Calculated annual average background aerosol surface area (μm^2 cm^{-3}) from the (a) AER model, (b) NSU model, (c) Italy model, and (d) Cambridge model. Also shown are (e) surface areas derived from SAGE II observations of April 1991 [*Yue et al.*, 1994], and (f) *WMO* [1993] background surface area recommendation.

years have shown that an EI(NO_x) of 5 is achievable [*Stolarski et al.*, 1995]. EI(H_2O) of 1230 is used in all calculations.

The EI of SO_2 is taken to be 0.4, based on projections that sulfur content in jet fuel will decline from its current average value of 0.8 [*Baughcum et al.*, 1994]. Because these 2-D models are not formulated to calculate tropospheric aerosols, we have not included sulfur emissions from subsonic aircraft or from HSCT aircraft below 13 km. The aircraft sulfur emissions amount to 2.4×10^{10} grams SO_2 per year deposited between 13 and 22 km altitude. At 45°N and 19 km, which represents the peak of HSCT traffic, sulfur emissions amount to about 30 molecules cm^{-3} s^{-1} of SO_2. If emissions are assumed to be 100% particles of 10 nm radius, this value represents about 90 particles cm^{-3} day^{-1}, corresponding to a surface area rate of increase of about 0.1 μm^2 cm^{-3} day^{-1}.

3.1. Surface Area Changes

Figure 2 shows the calculated change in the annual average aerosol surface area density due to emission of sulfur from HSCT aircraft, assuming that it remains SO_2 until mixing dilutes the plume to grid box size (assumption 1). The spatial variation of the perturbation corresponds to the geographical distribution of fuel usage, which is concentrated in the northern hemisphere. Maximum changes in surface area range from 0.1 μm^2 cm^{-3} in the Cambridge model to 0.2 μm^2 cm^{-3} in the Italy model, 0.3 μm^2 cm^{-3} in the AER model, and 0.5 μm^2 cm^{-3} in the NSU model. After the aircraft sulfur is mixed into the global grid box as SO_2, reaction with

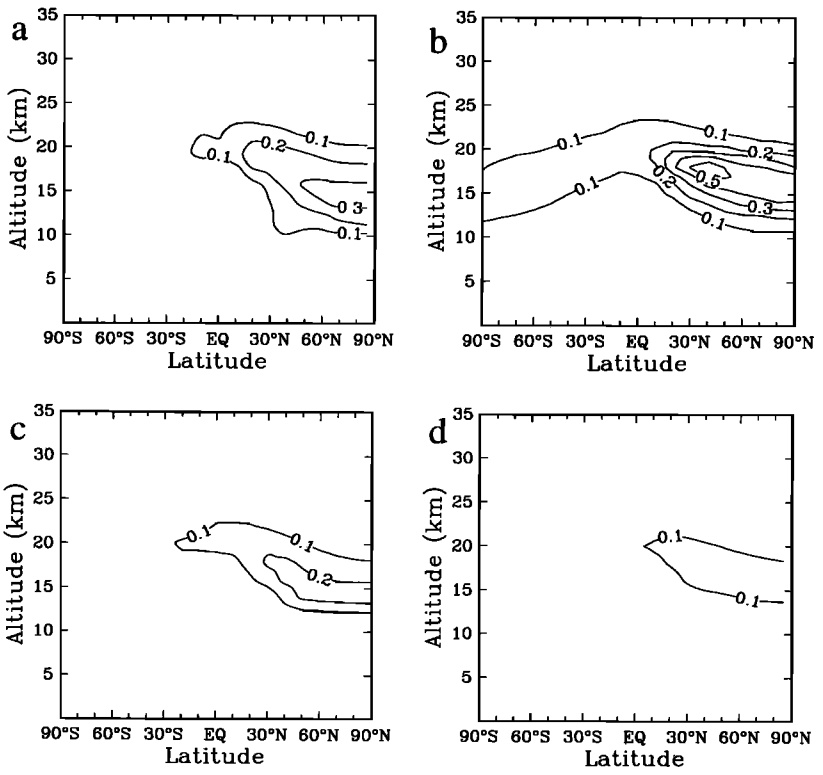

Figure 2. Calculated annual average increase in aerosol surface area (μm^2 cm^{-3}) due to HSCT emissions with EI(SO_2)=0.4, assumed emitted as SO_2 gas. Results are from (a) AER model, (b) NSU model, (c) Italy model, and (d) Cambridge model.

OH is the only pathway to produce H_2SO_4. Therefore model differences may reflect variations in calculated OH concentration, as well as the distribution of available sulfate particles on which gas phase H_2SO_4 may condense. As a percentage of the background surface area, calculated perturbations in the northern hemisphere lower stratosphere are up to 25% in the Italy model, up to 30% in the Cambridge model, up to 40% in the AER model, and up to 50% in the NSU model. The Cambridge and AER models show their largest percent change in the tropics because the calculated background is quite low there.

Increases in aerosol surface area under assumption 2, when 10% of the emitted sulfur is assumed to be converted to aerosol particles in the plume, are shown in Figure 3 for the four models. The aerosol particles generated in the aircraft plume are assumed to be of radius 10 nm (0.01 μm). This assumption is consistent with model calculations of the wake regime by *Fahey et al.* [1995] and *Danilin et al.* [1997]. Calculated maximum changes in aerosol surface area under this assumption are 0.4 μm^2 cm^{-3} for the AER and Cambridge models, 0.6 μm^2 cm^{-3} for the Italy model, and 0.8 μm^2 cm^{-3} for the NSU model. Corresponding percentage changes are 65% for the AER model and 75% for the Cambridge, Italy, and NSU models. The inclusion of aerosol particles in the emission scenario increases the surface area perturbation for each of the models, but the amount varies from 0.1 μm^2 cm^{-3} for the AER model to 0.4 μm^2 cm^{-3} for the Italy model.

Calculated increases in aerosol surface area under assumption 3, when all emissions are assumed to be particles, are shown in Figure 4. The maximum surface area increases are 1.0 μm^2 cm^{-3} in the Cambridge model, 1.5 μm^2 cm^{-3} in the AER model, 2.0 μm^2 cm^{-3} in the NSU model, and 2.5 μm^2 cm^{-3} in the Italy model. These perturbations are more than double those found under assumption 2 and represent increases of up to 200% over background for each model. The Italy model calculates as much as a 300% increase over the background surface area. Note that the area of maximum perturbation is more localized under assumption 3 than under the other two assumptions because aerosols are input directly along the flight tracks as small particles with high surface-to-volume ratio.

Differences in transport rates between the models appear to account for most of the intermodel differences in surface area perturbation. Relative changes in stratospheric aerosol mass among the four models mirror relative changes in surface area. The smaller calculated surface area (and aerosol mass) perturbations are related to shorter residence times and faster transport rates in the model stratosphere. The Cambridge model has the smallest increase in surface area under assumptions 1, 2, and 3 and uses an Eulerian transport scheme with faster advection and larger diffusion coefficients than

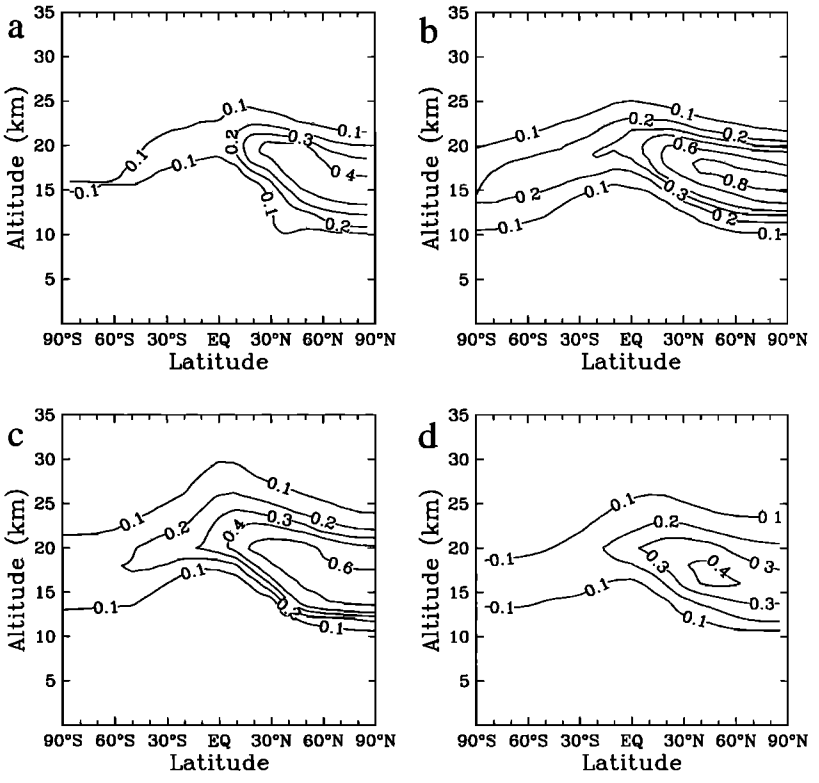

Figure 3. Calculated annual average increase in aerosol surface area (μm^2 cm^{-3}) due to HSCT emissions with EI(SO_2)=0.4, assumed emitted as 10% particles and 90% SO_2 gas. Results are from (a) AER model, (b) NSU model, (c) Italy model, and (d) Cambridge model.

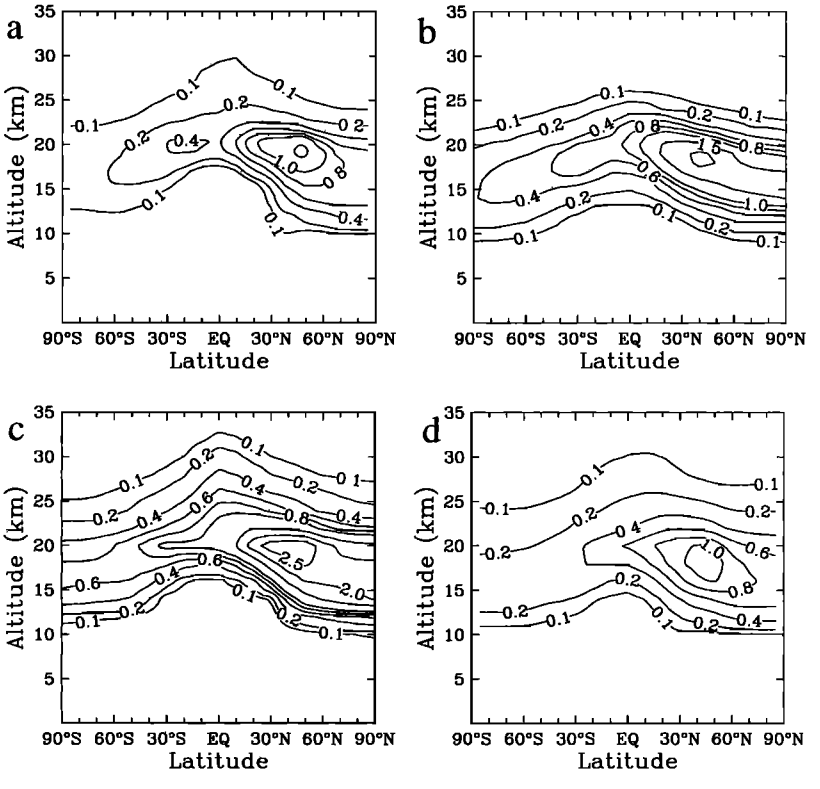

Figure 4. Calculated annual average increase in aerosol surface area (μm^2 cm^{-3}) due to HSCT emissions with EI(SO_2)=0.4, assumed emitted as 100% particles of 10 nm radius. Results are from (a) AER model, (b) NSU model, (c) Italy model, and (d) Cambridge model.

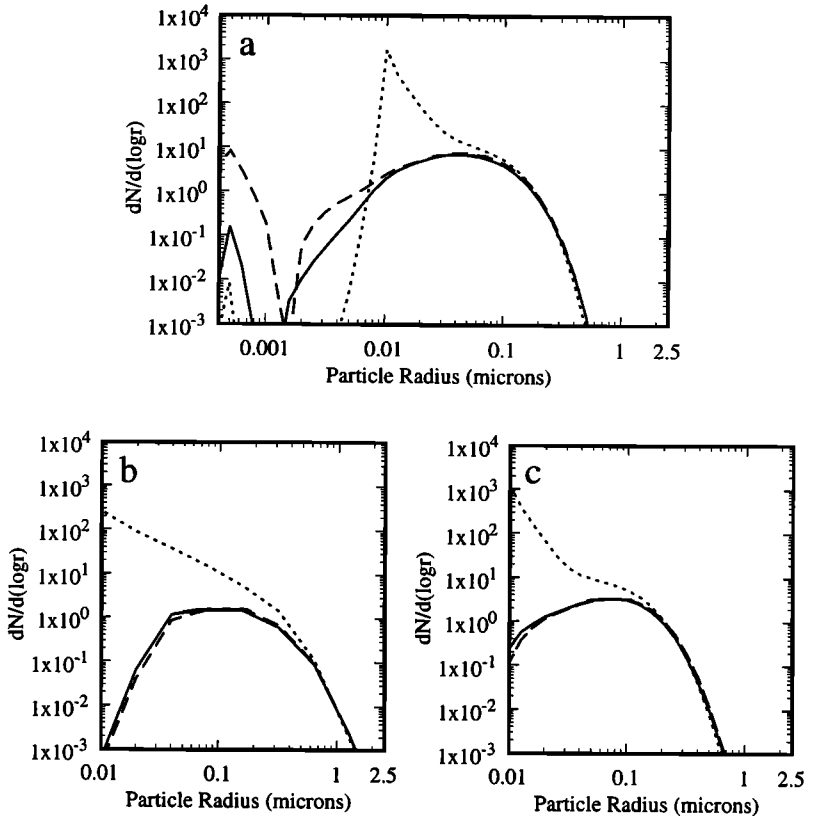

Figure 5. Calculated aerosol number density $dN/d(\log r)$ as a function of particle radius for the (a) AER, (b) Italy, and (c) Cambridge models. The solid line represents the background distribution, the dashed line represents a simulation including HSCT emissions of sulfur as SO_2 gas, and the dotted line represents a simulation including HSCT emissions of sulfur as 10 nm particles.

the other models. The Italy model has a small increase in surface area under assumption 1 but the largest increase in surface area under assumption 3. It uses a relatively slow transport rate, which yields a greater increase in stratospheric aerosol mass due to HSCT emissions. Surface area increases under assumption 1, however, also depend on the background particle size distribution. With the coarser resolution of aerosol sizes in the Italy model the background distribution is shifted toward larger particles. Condensation on larger particles provides a smaller surface area increase than does condensation on smaller particles.

To illustrate how the aerosol size resolution and calculated background aerosol distribution influence the HSCT surface area perturbation, we show in Figure 5 calculated aerosol size distributions for the AER, Italy, and Cambridge models under background and HSCT conditions at 45°N and 20 km in March. Under background conditions the AER model shows a maximum in number density at 0.04 μm radius, while the Italy and Cambridge models, which do not consider particles smaller than 0.01 μm, shows peak number densities at 0.08 and 0.06 μm, respectively. The Cambridge and AER models use a finer size resolution than the Italy model and show background size distributions that include more small particles and fewer large particles. The shape of the size distributions in the AER and Cambridge models are similar, though the total particle number density is smaller in the Cambridge model.

With addition of HSCT sulfur as gas phase SO_2 the Italy model shows a decrease in number density for particles less than 0.08 μm radius and an increase for particles greater than 0.08 μm. The Cambridge model results are similar, but decreases in number density are evident only for particles less than 0.03 μm. Such changes in particle number density are typical when condensation onto existing particles is the only mechanism for converting gas phase H_2SO_4 into aerosols. The AER model shows evidence for new particle production by nucleation, as the number of particles less than 0.001 μm is increased by addition of HSCT gas phase emissions. The gas phase sulfur emissions increase nucleation in the stratosphere by 150%, though only 6% of the emitted sulfur undergoes nucleation, while 94% condenses onto existing particles. With HSCT emissions as 100% particles, coagulation is the main process for interaction between the background distribution and the new particles. The AER and Cambridge models show similar size distributions for particles between 0.01 and 0.1 μm. The Italy models show a greater redistribu-

tion of injected sulfur into particle sizes between 0.01 and 1 μm. When the background distribution contains particles smaller than 0.01 μm, as in the AER model, these small particles preferentially coagulate with the injected 0.01 μm particles, somewhat reducing the surface area of the combined background/HSCT distribution in comparison with the distribution expected without this interaction. Note, however, that it is not possible to distinguish the relative importance of differences in transport and differences in aerosol size resolution on the basis of these calculations.

The sensitivity of these results to the assumed size of aerosol particles at plume breakup has been investigated with the AER and NSU models. Calculations were performed with particle sizes ranging from 0.4 nm to 80 nm. The maximum impact on aerosol surface area was found for particles in the 2.5 to 20 nm range. Smaller particles coagulate faster with background aerosols, reducing the surface area increase, and larger particles are removed more rapidly by sedimentation. Input of 80 nm particles resulted in less than half the surface area perturbation calculated for 10 nm particles under assumption 3. A calculation with 0.4 nm particles produced a peak aerosol surface area enhancement which was 25% less than that with 10 nm particles under assumption 3. A modeling study of the far-wake regime [*Danilin et al.*, 1997] indicated that the particle size distribution at 1 week after emission is sensitive to the wake dilution rate. By employing a very fast, a very slow, and an intermediate dilution rate, several possible particle size distributions were obtained, with peak number densities occurring between 4 and 20 nm. Our choice of 10 nm particles falls within this range and produces approximately the largest expected impact.

3.2. Ozone Changes

Calculated changes in annual average column ozone as a function of latitude due to emission of NO_x, H_2O, and sulfur from HSCT aircraft are shown in Figure 6 for each of the four models. Four results are shown for each model: the solid line represents aircraft emissions with EI(NO_x)=5 and no sulfur emissions, while the three dashed lines include sulfur emissions with EI(SO_2)=0.4 under assumptions 1, 2, and 3. Each model used its own calculated background aerosol surface area (those shown in Figure 1) for the subsonic case (used as the baseline) and the HSCT case without sulfur emissions. Without sulfur emissions, ozone column changes due to this HSCT scenario range from -0.1% to +0.2% near the equator and from 0% to -0.7% for middle and high latitudes. All models show more ozone depletion at high northern latitudes than at high southern latitudes as a result of the asymmetry of the HSCT source. The Italy model shows little change in column ozone between 30°S and 50°N and depletions of up to 0.3% at higher latitudes. The Cambridge model shows small ozone depletion in the tropics and up to 0.5% depletion near the north pole. Both the AER and NSU models show no ozone column change at the equator and 0.6% to 0.7% depletion near the north pole. Ozone column changes at the south pole are about -0.2% to -0.3% for all models.

With addition of sulfur emissions from HSCT aircraft, all models show greater ozone depletion, which increases with concurrent increases in aerosol surface area. Increasing aerosol surface area has two effects on the ozone impact of HSCT. It reduces the amount of NO_y in the active forms of NO and NO_2, thus decreasing the importance of the NO_x cycle to ozone loss and reducing the impact of aircraft-emitted NO_x. It also increases the amount of chlorine and HO_x in the active

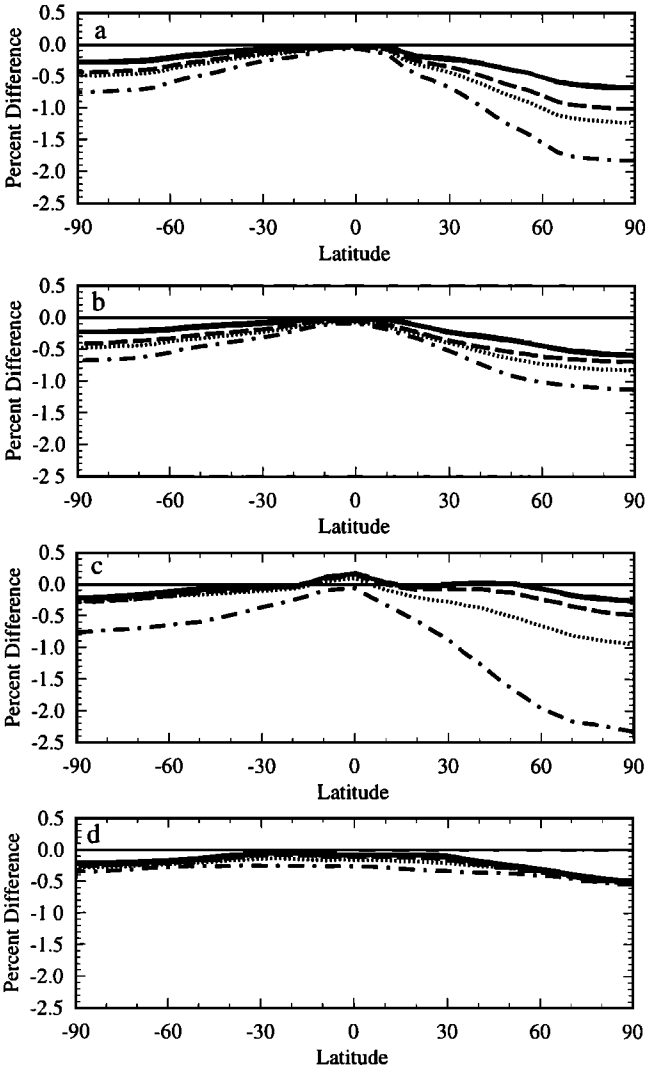

Figure 6. Calculated changes in annual average column ozone due to an HSCT emission scenario with EI(NO_x)=5, EI(H_2O)=1230, and different assumptions on sulfur emissions from the (a) AER model, (b) NSU model, (c) Italy model, and (d) Cambridge model. The solid line represents a case with no SO_2 emissions, the long dashed line represents EI(SO_2)=0.4 with assumption 1, the short dashed line represents EI(SO_2)=0.4 with assumption 2, and the dot-dashed line represents EI(SO_2)=0.4 with assumption 3. Background Cl_y is 3 ppbv.

forms of ClO and HO_2, leading to ozone depletion. For the EI(NO_x)=5 scenario the latter effect is more significant, and there is additional ozone depletion. The impact of sulfur emission on ozone column change is smallest in the tropics and greatest at northern high latitudes in all models except the Cambridge model. The additional ozone column depletion under assumption 1 is less than or equal to 0.3%. Further depletion under assumption 2 is only an additional 0.1-0.2% (compared with results under assumption 1) except for the Italy model, which calculates additional ozone depletion of 0.4% in the northern hemisphere. Under assumption 3 additional ozone depletion beyond that calculated under assumption 2 is up to 0.6% for the AER model, 0.3% for the NSU model, up to 1.4% for the Italy model, and 0.1% for the Cambridge model.

The Cambridge and Italy models show similar ozone column depletion under assumption 1. The Italy model, however, shows the largest depletion under assumption 3 (as much as 2.3% on an annual average basis), while the Cambridge model shows the smallest depletion under assumption 3 (only 0.5% at most). This difference is consistent with the differences in calculated aerosol surface area perturbation and treatment of heterogeneous chemistry. The AER and NSU models yield similar ozone responses to HSCT emissions with no fuel sulfur, but the AER model yields greater ozone depletion with fuel sulfur. Maximum annual average ozone column changes under assumption 3 are 1.1% for the NSU model and 1.8% for the AER model. The NSU model calculates a larger aerosol surface area perturbation than the AER model, but the AER model calculates a larger ozone response because it includes a temperature distribution. We can separate differences in calculated aerosol surface area from differences in calculated ozone depletion by using the calculated surface area density from various models in a single model. Use of the surface area density calculated by the Italy model under assumption 3 in the AER model results in maximum annual average ozone depletion of 2.5%. Use of the Cambridge model surface area calculated under assumption 3 in the AER model results in a maximum of 1.7% annual average ozone depletion.

To further emphasize the difference between assumption 1, with all sulfur emission as gas, and assumption 3, with all sulfur emission as particles, we examine in Figure 7 the calculated changes in ozone column as a function of latitude and season due to HSCT emissions with EI(NO_x)=5 for the AER, Italy, and Cambridge models. With emission of sulfur as all gas the AER model shows ozone loss across all of the extratropics, while the Italy model shows some ozone increase in spring from 30° to 50°N and in the tropics. The Cambridge model shows less than 0.3% ozone column depletion at all latitudes and seasons except poleward of 50° in summer and fall. With emission of sulfur as all particles, ozone reductions in the AER and Italy models are dramatic, occurring at all latitudes and seasons. With these models, ozone depletion is greatest at high northern latitudes in spring, with more than 2% ozone depletion between 60°N and 90°N in March and April. Ozone depletion in the southern hemisphere high latitudes approaches 1% in spring. The midlatitudes and tropics show little seasonal contrast. The Cambridge model shows only modest changes in ozone depletion due to particle rather than gas phase sulfur emissions, with the greatest change in the tropics and at high latitudes in spring.

Figure 8 shows profiles of ozone changes at 45°N in June for the four models with no sulfur emissions and with sulfur emissions under the three assumptions for EI(NO_x)=5. For all of the models, HSCT emissions without sulfur produce an ozone increase in the troposphere and an ozone decrease in the middle stratosphere above 20 km, but the response in the lower stratosphere (10-20 km) varies markedly between models. This variation reflects the sensitivity of ozone in this region to catalytic loss by the HO_x, NO_x, and ClO_x cycles and to transport. HSCT emissions add H_2O, and therefore HO_x, and NO_x, increasing ozone loss by their respective catalytic cycles. But NO_x emissions also tend to reduce the HO_x and ClO_x cycles by forming HNO_3 and $ClONO_2$. The increase in the NO_x cycle appears to dominate the ozone response in this region in the AER and NSU models, while reductions in the HO_x and ClO_x cycles dominate in the Cambridge and Italy models. In this sensitive region of the stratosphere, differences in model formulations of both chemistry and transport substantially influence calculated changes in ozone, leading to model differences in the sign and the magnitude of the ozone response to HSCT between 10 and 20 km.

When emissions of sulfur are also considered, all models predict a more negative response to HSCT emissions in the troposphere and lower stratosphere. The sensitivities vary, however. At 15 km the difference in the percent ozone change between the scenario with no sulfur emissions and that with sulfur emissions as 100% particles is 1.1% in the Cambridge model, 1.2% in the NSU model, 2.7% in the AER model, and 5.5% in the Italy model. In the middle stratosphere, where the NO_x cycle constitutes a large fraction of the total ozone loss, all models calculate less ozone loss due to HSCT sulfur emissions. The altitude at which increases in aerosol surface area begin to cause ozone enhancement rather than depletion varies from 20 km in the NSU model to 24 km in the Italy model and has some dependence on absolute surface area. The Cambridge model shows the greatest ozone increase in the middle stratosphere due to aerosol emissions, which largely offsets the calculated depletion at lower altitudes and accounts for the modest change in column ozone due to aerosol emissions.

Figure 9 shows changes in annual average ozone column due to HSCT emissions for a scenario with EI(NO_x)=15. The Cambridge model did not calculate this scenario, so only three model results are shown.

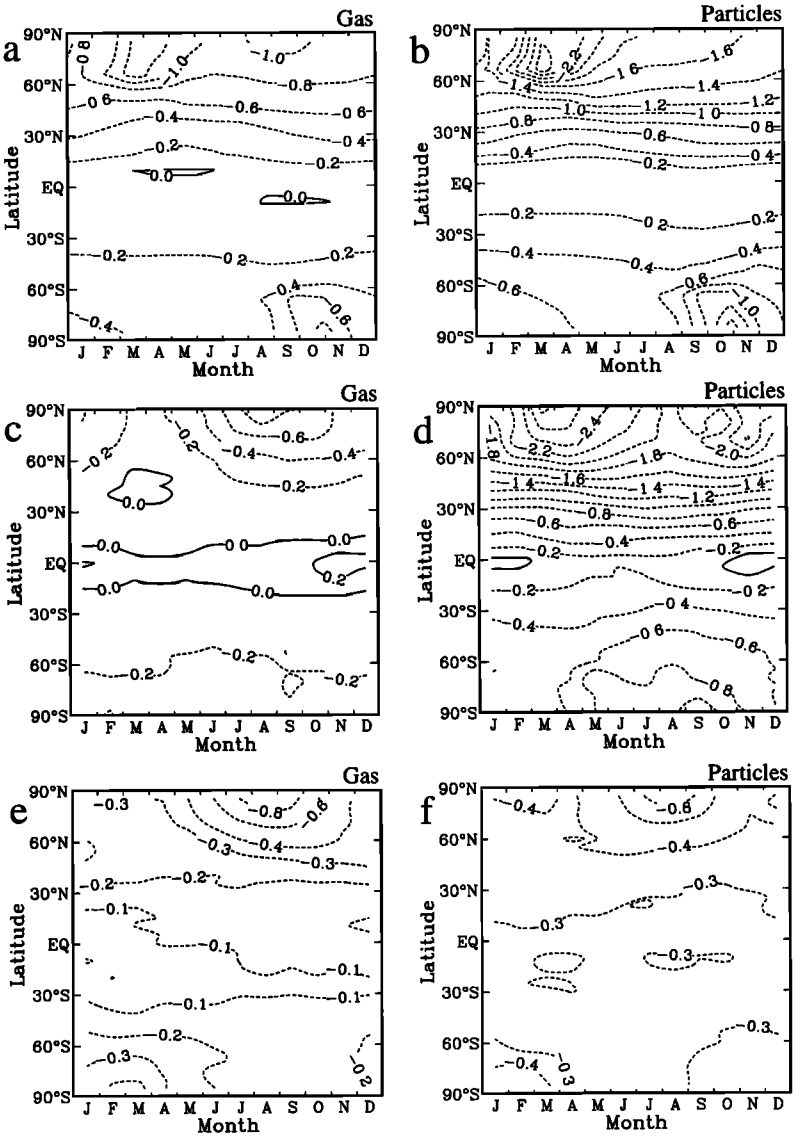

Figure 7. Calculated percent change in column ozone as a function of latitude and season due to HSCT emissions with EI(NO_x)=5, EI(H_2O)=1230, and EI(SO_2)=0.4 for the (a, b) AER, (c, d) Italy, and (e, f) Cambridge models under assumptions (left) 1 and (right) 3. The background Cl_y is 3 ppbv.

With sulfur emissions omitted the ozone response is significantly larger than that for EI(NO_x)=5. The response is due primarily to increases in NO_x catalytic loss of ozone. The response to sulfur emissions is quite different from that seen with EI(NO_x)=5. While the southern hemisphere still shows increased ozone depletion with increasing surface area, the northern hemisphere shows a variety of responses among the models. The AER and Italy models show only a small response in the northern hemisphere to sulfur emissions under assumptions 1 and 2 but show a substantial negative response to sulfur emissions under assumption 3. In the NSU model the sulfur emissions reduce ozone depletion in the northern hemisphere. Sulfur emissions can "buffer" or reduce the effects of high NO_x emissions by aircraft, since heterogeneous reactions on the increased surface area reduce the amount of emitted NO_x that remains in active forms. The NSU model does, however, show greater ozone depletion under assumption 3 than under assumption 1 or 2.

Changes in June ozone profile at 45°N for the three models with EI(NO_x)=15 are shown in Figure 10. All models show substantial ozone increases in the troposphere due to emission of NO_x, but varying from 1.7% in the NSU model to 2.5% in the AER model and 4.0% in the Italy model. The tropospheric ozone increase is somewhat reduced by sulfur emissions. Note, however, that tropospheric ozone changes contribute little to the total column response. In the lower stratosphere the AER and Italy models show enhanced ozone depletion due to sulfur emissions, while the NSU model shows reduced ozone depletion. It is likely that the NSU model

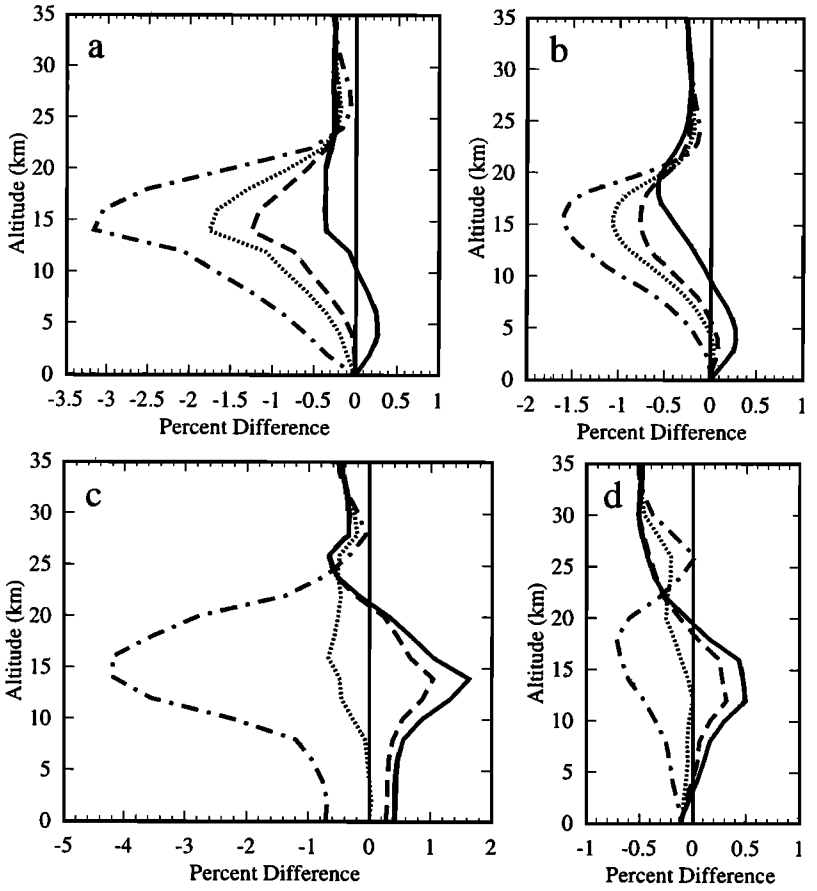

Figure 8. Calculated percent change in ozone due to HSCT emissions with EI(NO_x)=5, EI(H_2O)=1230, and different assumptions on sulfur emissions in June at 45°N for (a) AER model, (b) NSU model, (c) Italy model, and (d) Cambridge model. The solid line represents a case with no SO_2 emissions, the long dashed line represents EI(SO_2)=0.4 with assumption 1, the short dashed line represents EI(SO_2)=0.4 with assumption 2, and the dot-dashed line represents EI(SO_2)=0.4 with assumption 3. Background Cl_y is 3 ppbv.

would show less of a positive response in this region if a temperature distribution were included and the effect of heterogeneous reactions were enhanced.

Table 1 lists percent changes in column ozone at 45°N and on a global average basis for the AER, NSU, Italy, and Cambridge models due to an HSCT fleet with NO_x emission indices of 5 and 15. Global ozone changes are about one half to two thirds of the changes at 45°N for most scenarios. Calculated changes in global ozone are less than or equal to 0.2% depletion with EI(NO_x)=5 and no sulfur emissions but as much as 0.8% with sulfur emissions as 100% particles. Global ozone changes with EI(NO_x)=15 are up to 0.4% depletion without sulfur emissions and up to 0.5% depletion with sulfur emissions as 100% particles. Comparing the EI(NO_x)=5 and the EI(NO_x)=15 scenarios, we see much larger ozone depletion for EI(NO_x)=15 without sulfur emissions from aircraft, but with sulfur emissions as 100% particles, ozone depletion is larger for EI(NO_x)=5. Thus attempts to control NO_x emissions from aircraft without concomitant reductions in fuel sulfur may not yield desired controls on ozone depletion.

4. Sensitivity Studies

4.1. Temperature Probability Distribution

To illustrate the importance of a temperature probability distribution in the calculation of ozone changes induced by HSCT emissions, we show in Figure 11 results from the AER and Italy models without a temperature distribution for the EI(NO_x)=5 scenario. These ozone column changes as a function of latitude and season can be compared with those shown in Figure 7, which include the distribution. Except for the Italy model with gas phase sulfur emissions, ozone column changes are smaller without the distribution, particularly for the case with 100% particle emissions. The seasonality of ozone depletion is also changed, with maximum depletion found in fall without a temperature distribution and in spring with a temperature distribution. Northern midlatitude ozone depletion is strongly affected as well. By including a temperature distribution, annual average ozone depletion at 45°N changes from 0.81% to 1.14% in the AER model with particle emissions and from 0.90% to 1.45% in the Italy model with particle emissions. Ozone column depletion results for the

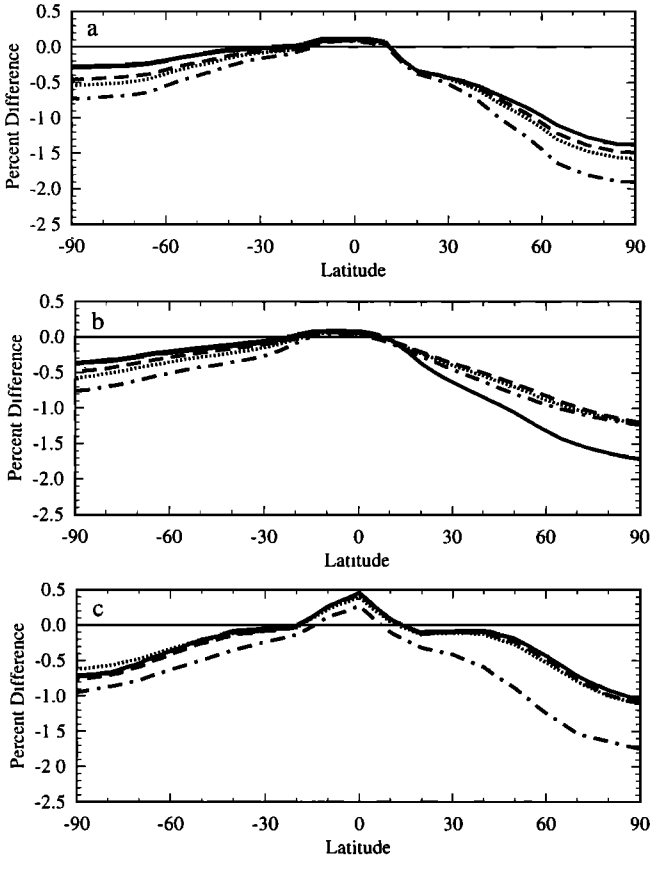

Figure 9. Calculated changes in annual average column ozone due to an HSCT emission scenario with EI(NO_x)=15, EI(H_2O)=1230, and different assumptions on sulfur emissions from the (a) AER model, (b) NSU model, and (c) Italy model. The solid line represents a case with no SO_2 emissions, the long dashed line represents EI(SO_2)=0.4 with assumption 1, the short dashed line represents EI(SO_2)=0.4 with assumption 2, and the dot-dashed line represents EI(SO_2)=0.4 with assumption 3. Background Cl_y is 3 ppbv.

EI(NO_x)=5 scenario for the AER and NSU models are quite similar without a temperature distribution in either model.

For scenarios with particle emissions, and thus greatly enhanced aerosol surface area distributions, the effect of including a temperature distribution for calculation of heterogeneous reaction rates is quite important, resulting in a doubling of the calculated ozone depletion in both polar regions in spring. Reactions (3) and (4), involving reactions with HCl on sulfate aerosol surfaces, are responsible for most of this sensitivity, with reaction (3) accounting for about two thirds of the effect and reaction (4) accounting for the remainder. The Cambridge model also uses a temperature distribution but does not calculate greatly enhanced ozone depletion with HSCT particle emissions, possibly as a result of the cruder parameterization of reaction (3) and omission of reaction (4). Our results imply that use of a temperature distribution in 2-D models and of accurate temperature fields and fluctuations in box and trajectory models is important for calculating ozone and ozone trends, especially under conditions of perturbed stratospheric sulfur, such as following volcanic eruptions. This sensitivity has been noted previously by *Murphy and Ravishankara* [1994], *Borrmann et al.* [1997], and *Michelsen et al.* [1997].

4.2. Polar Stratospheric Clouds

The effect of including polar stratospheric clouds (PSCs) in a 2-D model along with HSCT sulfur emissions has been investigated by the Italy model. The method of treating PSCs is described by *Pitari et al.* [1993] and involves heterogeneous nucleation of NAT particles on sulfate aerosols and nucleation of ice particles on NAT particles. The processes of condensation, evaporation, and sedimentation are also modeled. As shown in the paper by *Pitari et al.* [1993], the inclusion of PSC aerosols has the net effect of mitigating the ozone column decrease produced by supersonic aircraft. The net column change is the result of two opposite ozone anomalies, with the positive one below about 15-20 km altitude where ClO_x and HO_x catalytic cycles have a larger impact on ozone relative to the NO_x cycle.

The NO_2 increase resulting from direct aircraft emission lowers the $ClO/ClONO_2$ ratio, thus producing a ClO decrease with respect to the background atmosphere and also removing more OH via the three-body reaction forming HNO_3. The relative weight of the associated ozone increase is larger if the background stratospheric amount of NO_x is smaller, as is the case when PSC particles are present and a net redistribution of NO_y is produced by particle sedimentation. Chlorine processing by heterogeneous chemical reactions on PSC surfaces is another effect to be taken into account. If the surface area were kept constant, no additional ozone changes would be produced by the aircraft emissions. However, both NO_x and SO_x emissions from HSCT may increase the PSC particle surface available for heterogeneous chemistry by increasing the saturation ratios of HNO_3 and H_2SO_4 and then speeding up the processes of particle growth and nucleation.

Calculations with the Italy model including PSCs for both the baseline simulation and the HSCT simulation with EI(NO_x)=5 show substantially less ozone depletion than calculations without PSCs. With the effect of a temperature distribution also included, calculated annual average changes in column ozone poleward of 40°N are 0.0% with sulfur emissions treated as SO_2 gas and -1.0% with sulfur emissions treated as 100% particles. Corresponding ozone changes without PSCs are -0.3% and -2.0%. The ozone response to HSCT emissions is less sensitive to a temperature distribution with PSCs included because reaction probabilities of $ClONO_2$ and HOCl on PSC surfaces are assumed to be temperature independent. Results of HSCT sensitivity to PSCs in 2-D models is expected to be sensitive to model formulation, and indeed, among 2-D models that have per-

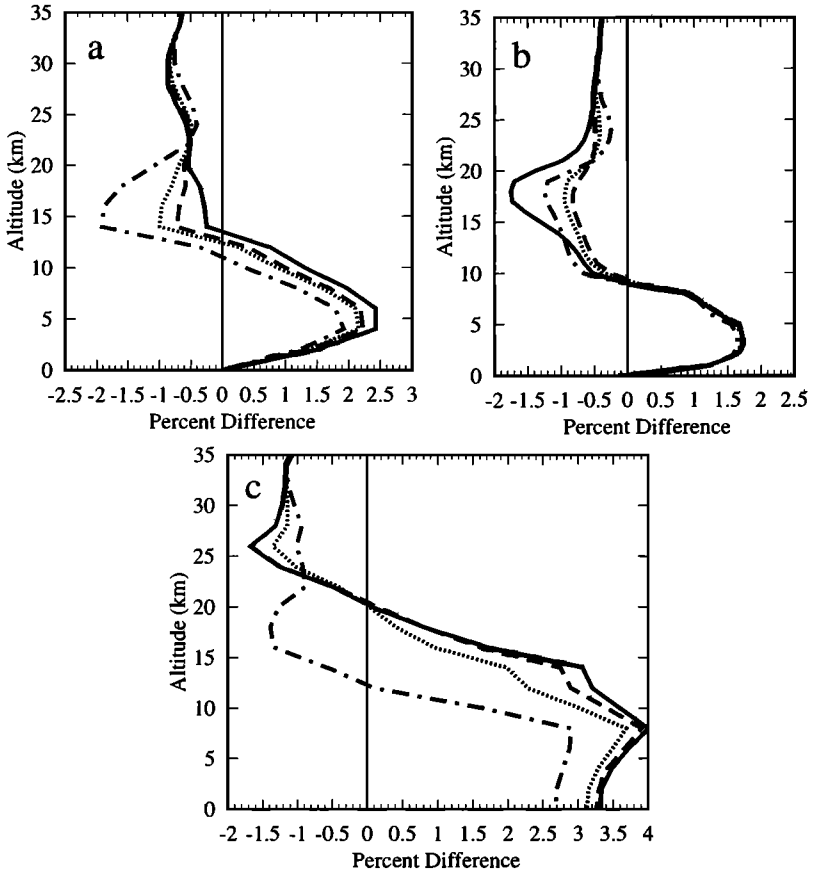

Figure 10. Calculated percent change in ozone due to HSCT emissions with EI(NO_x)=15, EI(H_2O)=1230, and different assumptions on sulfur emissions in June at 45°N for (a) AER model, (b) NSU model, and (c) Italy model. The solid line represents a case with no SO_2 emissions, the long dashed line represents EI(SO_2)=0.4 with assumption 1, the short dashed line represents EI(SO_2)=0.4 with assumption 2, and the dot-dashed line represents EI(SO_2)=0.4 with assumption 3. Background Cl_y is 3 ppbv.

formed similar experiments, no clear consensus has been reached [*Stolarski et al.*, 1995].

4.3. Background Cl_y

The sensitivity of the HSCT ozone response to Cl_y is important because it is expected that Cl_y will decrease in the future as the atmosphere responds to reduced emissions of CFCs and other chlorine-bearing compounds. A Cl_y concentration of about 2.0 ppbv is forecast for 2050 [*WMO*, 1995]. Figure 12 shows calculated annual average ozone column changes due to HSCT emissions with EI(NO_x)=5 and 2 ppbv of Cl_y

Table 1. Calculated Change in Annual Average Ozone Column Due to Emissions From a Mach 2.4 HSCT Fleet in 2015

	AER		NSU		Italy		Cambridge	
Sulfur Emission*	45°N	Global	45°N	Global	45°N	Global	45°N	Global
				EI(NO_x)=5				
None	−0.35%	−0.21%	−0.32%	−0.16%	0.02%	−0.02%	−0.22%	−0.14%
0% particles	−0.57%	−0.33%	−0.50%	−0.27%	−0.11%	−0.09%	−0.26%	−0.17%
10% particles	−0.72%	−0.40%	−0.59%	−0.32%	−0.44%	−0.23%	−0.27%	−0.21%
100% particles	−1.14%	−0.63%	−0.83%	−0.44%	−1.45%	−0.77%	−0.36%	−0.30%
				EI(NO_x)=15				
None	−0.65%	−0.30%	−0.94%	−0.35%	−0.14%	−0.12%		
0% particles	−0.71%	−0.36%	−0.57%	−0.25%	−0.17%	−0.15%		
10% particles	−0.75%	−0.39%	−0.62%	−0.29%	−0.20%	−0.15%		
100% particles	−0.95%	−0.52%	−0.71%	−0.36%	−0.74%	−0.46%		

The background inorganic chlorine amount for 2015 was 3 ppbv.

*Sulfur emissions with EI(SO_2)=0.4 are treated as 100% gas, 90% gas and 10% aerosol particles of 10 nm radius, or 100% aerosol particles of 10 nm radius. A case with no sulfur emissions is also shown.

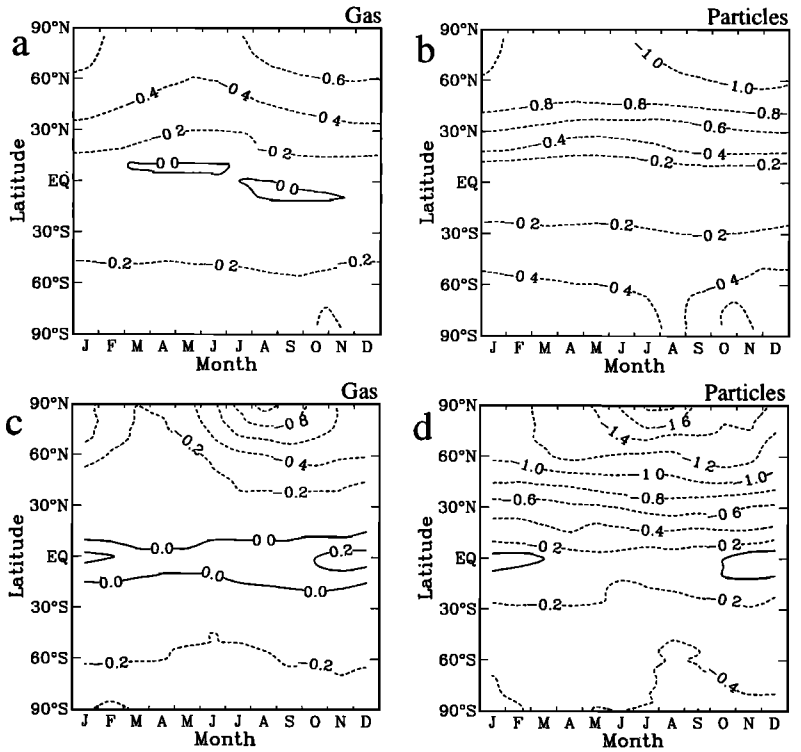

Figure 11. Calculated percent change in column ozone as a function of latitude and season due to HSCT emissions with EI(NO_x)=5, EI(H_2O)=1230, and EI(SO_2)=0.4 for the (a, b) AER and (c, d) Italy models under assumptions (left) 1 and (right) 3, omitting the effect of a temperature distribution on heterogeneous reaction rates. To be compared with Figure 7 including a temperature distribution. The background Cl_y is 3 ppbv.

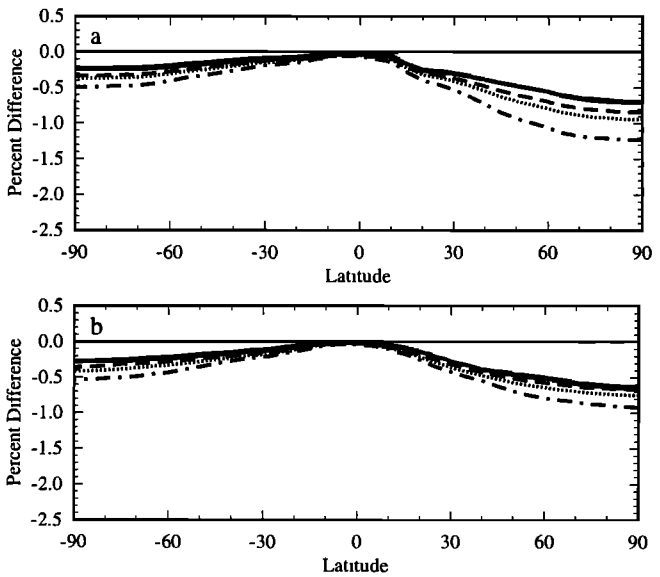

Figure 12. Calculated changes in annual average column ozone due to an HSCT emission scenario with EI(NO_x)=5, EI(H_2O)=1230, and different assumptions on sulfur emissions from the (a) AER model and (b) NSU model. The solid line represents a case with no SO_2 emissions, the long dashed line represents EI(SO_2)=0.4 with assumption 1, the short dashed line represents EI(SO_2)=0.4 with assumption 2, and the dot-dashed line represents EI(SO_2)=0.4 with assumption 3. Background Cl_y is 2 ppbv. To be compared with Figures 6a and 6d.

for the AER and NSU models. Without sulfur emissions the calculated ozone depletion is slightly larger in midlatitudes for 2 ppbv of Cl_y than for 3 ppbv of Cl_y. With emission of sulfur from aircraft, ozone depletion is increased, but by a lesser amount than that seen with 3 ppbv of Cl_y.

Figure 13 shows calculated annual average ozone column changes with EI(NO_x)=15 and 2 ppbv of background Cl_y for the same models. Again, calculated ozone depletion is larger for 2 ppbv of Cl_y than for 3 ppbv of Cl_y without sulfur emissions. This effect is due to reduced production of $ClONO_2$ when NO_x is emitted by aircraft in a low-chlorine environment. Northern hemisphere ozone depletion was increased by sulfur emission with 3 ppbv of Cl_y in the AER model but is unaffected by sulfur emissions with 2 ppbv of Cl_y. In the NSU model, ozone depletion in the northern hemisphere was reduced by sulfur emission with 3 ppbv of Cl_y, and with 2 ppbv of Cl_y it is reduced even further.

Table 2 lists calculated ozone column change at 45°N and global average ozone column change with EI(NO_x)=5 and 15 and 2 ppbv of Cl_y. With EI(NO_x)=5 and emission of sulfur as 100% particles (assumption 3), the calculated ozone depletion at 45°N from the AER model is 1.14% with 3 ppbv of Cl_y and 0.85% with 2 ppbv of Cl_y. From the NSU model, calculated ozone depletion at 45°N is 0.83% with 3 ppbv of Cl_y and 0.62% with 2 ppbv of Cl_y. With EI(NO_x)=15 and sulfur emis-

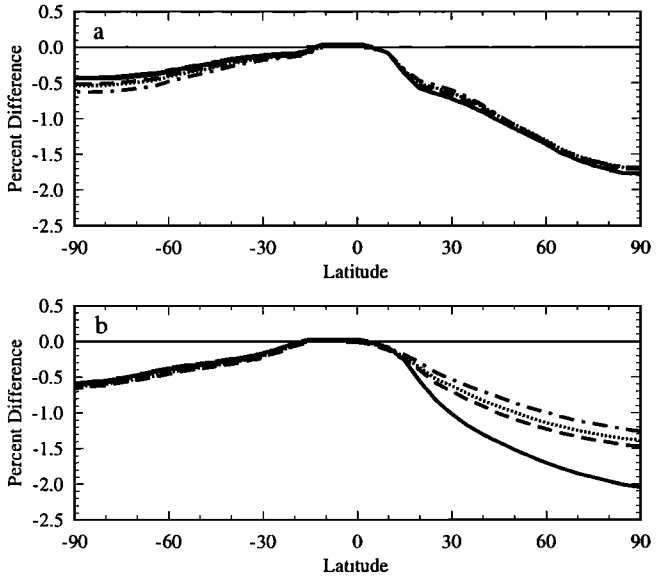

Figure 13. Calculated changes in annual average column ozone due to an HSCT emission scenario with EI(NO_x)=15, EI(H_2O)=1230, and different assumptions on sulfur emissions from the (a) AER model and (b) NSU model. The solid line represents a case with no SO_2 emissions, the long dashed line represents EI(SO_2)=0.4 with assumption 1, the short dashed line represents EI(SO_2)=0.4 with assumption 2, and the dot-dashed line represents EI(SO_2)=0.4 with assumption 3. Background Cl_y is 2 ppbv. To be compared with Figures 9a and 9b.

sions as particles, ozone column changes are about the same with 2 ppbv of Cl_y as with 3 ppbv of Cl_y.

4.4. $BrONO_2$ + H_2O Heterogeneous Reaction

Another sensitivity that we consider is the effect of including the heterogeneous reaction

$$BrONO_2 + H_2O \rightarrow HNO_3 + HOBr \quad (5)$$

on sulfate aerosols. This reaction is included in the NSU results presented above with a reaction probability (γ) of 0.4 based on the measurements of *Hanson and Ravishankara* [1995]. More recent measurements of this reaction have provided a γ which is a function of temperature and water activity [*Hanson et al.*, 1996]. Values of γ are as large as 0.8 for aerosols with acid weight percent of less than 70%, which occurs in the polar regions, though values of about 0.4 are still found over most of the stratosphere. This heterogeneous reaction has the effect of increasing active HO_x, ClO_x and BrO_x, mainly as a result of HOBr photolysis [*Randeniya et al.*, 1996], leading to enhanced ozone depletion.

AER model results including reaction (5) and using the parameterization of *Hanson et al.* [1996] are shown in Figure 14 for EI(NO_x) of 5 and 15. Compared with calculations that omit this reaction (see Figures 6a and 9a), ozone column changes are smaller without sulfur emissions, especially for EI(NO_x)=15. Sulfur emissions cause a greater perturbation with reaction (5) than without it. With EI(NO_x)=5 and sulfur emissions as 100% particles, calculated ozone depletion is 1.3% at 45°N with a global average ozone depletion of 0.7%. This is 20% more depletion than that without reaction (5).

4.5. Background Aerosol Loading

Variations in background aerosol amount have been found to affect calculated ozone change due to HSCT emissions [*Weisenstein et al.*, 1993]. There is uncertainty regarding the true "nonvolcanic" aerosol levels in the stratosphere, since periods free from volcanic influence have been seen only rarely in the past two decades [*Hitchman et al.*, 1994], most recently in 1979 [*Thomason et al.*, 1997]. The total stratospheric sulfur mass estimated for 1979 by *Kent and McCormick* [1984] was 570 kt. Models employing OCS photolysis as the major

Table 2. Calculated Change in Annual Average Ozone Column Due to Emissions From a Mach 2.4 HSCT Fleet in 2050

	AER		NSU	
Sulfur Emission*	45°N	Global	45°N	Global
	EI(NO_x)=5			
None	−0.43%	−0.24%	−0.42%	−0.20%
0% particles	−0.55%	−0.31%	−0.47%	−0.23%
10% particles	−0.63%	−0.35%	−0.52%	−0.27%
100% particles	−0.85%	−0.46%	−0.62%	−0.33%
	EI(NO_x)=15			
None	−1.03%	−0.51%	−1.41%	−0.55%
0% particles	−0.98%	−0.51%	−1.01%	−0.44%
10% particles	−0.97%	−0.51%	−0.91%	−0.41%
100% particles	−0.96%	−0.52%	−0.78%	−0.35%

The background inorganic chlorine amount for 2050 was 2 ppbv. Other long-lived trace species were retained at their 2015 levels.

*Sulfur emissions with EI(SO_2)=0.4 are treated as 100% gas, 90% gas and 10% aerosol particles of 10 nm radius, or 100% aerosol particles of 10 nm radius. A case with no sulfur emissions is also shown.

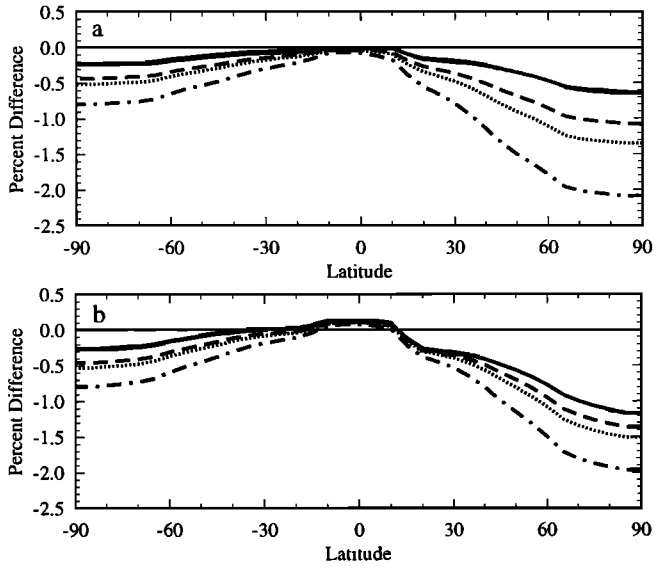

Figure 14. Calculated changes in annual average column ozone from the AER model due to an HSCT emission scenario with (a) EI(NO_x)=5 and (b) EI(NO_x)=15 and including the heterogeneous reaction $BrONO_2+H_2O$. The solid line represents a case with no SO_2 emissions, the long dashed line represents EI(SO_2)=0.4 with assumption 1, the short dashed line represents EI(SO_2)=0.4 with assumption 2, and the dot-dashed line represents EI(SO_2)=0.4 with assumption 3. Background Cl_y is 3 ppbv. To be compared with Figures 6a and 9a.

source of stratospheric sulfate are found to contain only about half this amount [*Chin and Davis*, 1995; *Weisenstein et al.*, 1997].

Deep tropospheric convection has been found to have a large effect on calculations of upper tropospheric SO_2 concentration [*Chatfield and Crutzen*, 1984; *Langner and Rodhe*, 1991] and potentially on stratospheric aerosol loading [*Weisenstein et al.*, 1997]. This process has been accounted for in the AER model by imposing an SO_2 concentration of 40 pptv in the tropical middle and upper troposphere [*Weisenstein et al.*, 1997] and leads to a factor of 5 increase in aerosol mass density and a factor of 2 increase in surface area density in the tropical lower stratosphere. Total stratospheric aerosol mass roughly doubles. We will present results for the HSCT impact using a "high background" aerosol surface area obtained from the AER model employing enhanced upper tropospheric SO_2.

Changes in calculated surface area due to HSCT emission of sulfur are smaller with the "high background" model. Increases in aerosol surface area density are reduced by 25-30% in relation to the results shown for the AER model in Figures 2-4. The percentage change over background is significantly less, especially in the low latitudes where most of the background surface area increase occurs. Calculated changes in ozone with high background sulfur and reaction (5) included are shown in Figure 15. The predicted ozone column change due to HSCT emissions is smaller at higher aerosol levels, both with and without sulfur emissions. With EI(NO_x)=5 the increased background aerosol surface area results in reductions in HSCT ozone column depletion at 45°N from -1.3% to -1.0% with sulfur emissions as 100% particles. With EI(NO_x)=15 the changes are larger, reducing ozone column depletion at 45°N from -0.5% to -0.1% without sulfur emission and from -1.0% to -0.6% with sulfur emissions as 100% particles. Following this logic, we can argue that during times of volcanic enhancement of the aerosol layer, HSCT emission of NO_x will lead to smaller ozone depletion, and the effect of sulfur emissions from aircraft will be reduced.

5. Summary and Conclusions

Four independently formulated two-dimensional models of trace species and sulfate aerosols have been applied to predict the effect of HSCT emissions on the stratospheric aerosol layer and on ozone. Model-predicted changes in aerosol surface area vary by a factor of 3 among the models for identical sulfur emissions. The main cause of model differences appears to be transport, which directly affects the residence time of the emitted sulfur and thus the magnitude of the surface area perturbation. However, the transport rate affects the background calculated surface area as well, and thus percentage perturbations are fairly consistent

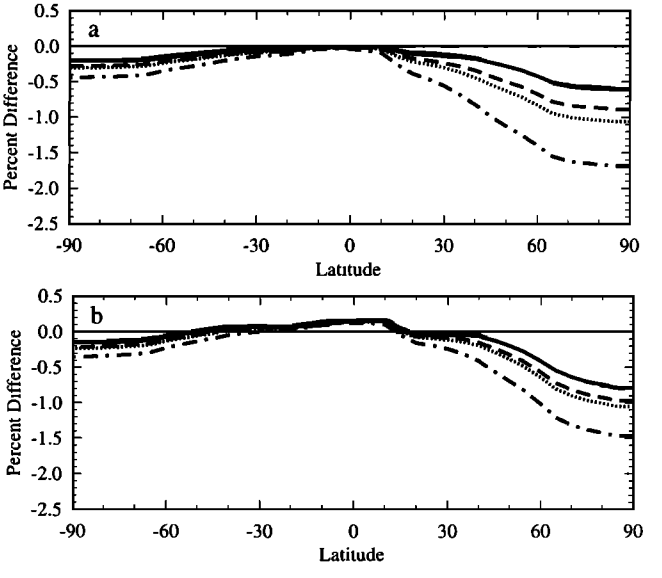

Figure 15. Calculated changes in annual average column ozone from the AER model due to an HSCT emission scenario with (a) EI(NO_x)=5 and (b) EI(NO_x)=15 for high background aerosol (see text) and including the $BrONO_2+H_2O$ reaction. The solid line represents a case with no SO_2 emissions, the long dashed line represents EI(SO_2)=0.4 with assumption 1, the short dashed line represents EI(SO_2)=0.4 with assumption 2, and the dot-dashed line represents EI(SO_2)=0.4 with assumption 3. Background Cl_y is 3 ppbv. To be compared with Figure 14.

among the models. When sulfur emissions are assumed to be in the form of gas phase SO_2, maximum increases in aerosol surface area range from 25% to 50% above their respective calculated background amounts. When 10% of the sulfur is assumed to be in particles of 10 nm radius, surface area increases are greater, up to 65% or 75%. When all sulfur is assumed emitted as particles, surface area increases are much greater, up to 200% or 300%. The conclusion of *Weisenstein et al.* [1996] that emission of sulfur by aircraft, if it is converted to particles within the wake, could strongly perturb stratospheric aerosol concentrations is supported by all four models used in this study.

The models show larger variations in ozone response to HSCT. This finding is to be expected because the ozone response is sensitive to the partitioning of HO_x, NO_x, ClO_x, and BrO_x radicals, to transport rates, and to the background aerosol surface area. The balance between these competing processes, unfortunately, generally depends on model formulation. There is no consensus on the best way to formulate a numerical model of atmospheric ozone. Even with perfect knowledge of the atmosphere, modelers would be forced to make compromises in constructing models to keep the computational requirements modest. We will treat variations in ozone response between the models as sensitivities to model formulation. Where qualitative consensus exist among the models, we will draw more robust conclusions regarding ozone response to HSCT.

All models agree with the conclusion of *Weisenstein et al.* [1996] that for the HSCT scenario with EI(NO_x)=5, which represents a very modest emission of NO_x, aircraft emission of sulfur will increase ozone depletion. This increase is due to increased heterogeneous processing on the enhanced aerosol layer, increasing ozone loss due to the HO_x and ClO_x catalytic cycles. Ozone depletion is largest if all sulfur is assumed emitted as particles. With this assumption, annual average ozone depletion at 45°N is calculated to be 1.1% for the AER model, 0.8% for the NSU model, 1.5% for the Italy model, and 0.4% for the Cambridge model with 3 ppbv of Cl_y. When EI(NO_x) is increased to 15, the models' calculated responses to emission of sulfur differ. This variable sensitivity can be understood as differences in the relative importance of NO_x catalytic loss of ozone (which is reduced by added sulfur) and HO_x and ClO_x catalytic loss of ozone (which is increased by added sulfur) in each model.

A number of model sensitivities are explored to see how the ozone response to HSCT emissions may vary under different conditions or with additional model parameterizations. An important result of these model calculations is that inclusion of a temperature distribution in 2-D models to account for deviations from the zonal mean temperature can significantly increase calculated ozone depletion due to HSCT emissions, especially when sulfur emissions are included. We recommend that use of a temperature probability distribution become a standard part of 2-D models, as it accounts for some important processes that are otherwise neglected and to which ozone is sensitive. Introduction of PSCs into the Italy model leads to smaller ozone depletion due to HSCT emissions, though this result is expected to be model dependent. With background Cl_y reduced from 3 ppbv to 2 ppbv, ozone depletion due to NO_x emission alone is increased, but ozone depletion due to sulfur emissions is reduced (with EI(NO_x)=5) or reversed (with EI(NO_x)=15). Inclusion of the heterogeneous reaction $BrONO_2+H_2O$ on sulfate aerosols leads to a slight reduction in ozone depletion without HSCT sulfur emissions and an increase in ozone depletion with sulfur emissions. This reaction should be included in future modeling studies. Increasing the background aerosol surface area leads to less ozone depletion due to HSCT NO_x emissions and less ozone depletion due to HSCT sulfur emissions.

The recommendation for future modeling studies of HSCT impact on ozone is that sulfur emissions must be included in assessment calculations, and knowledge of chemical and microphysical processes within the plume and far wake are crucial for accurate modeling. The fractional conversion of emitted sulfur to aerosol particles depends on processes within the engine, nozzle, and near-field plume [*Kärcher and Fahey,* 1997; *Brown et al.,* 1996b], and the resulting particle size distribution depends on dilution within the far wake [*Danilin et al.,* 1997]. The fractional conversion is bracketed in this study by 10% and 100% conversion, based on direct measurements in the Concorde plume [*Fahey et al.,* 1995]. Because the aerosol instrument did not measure particles smaller than 0.08 μm diameter and models predict a large number of such particles, the actual conversion is likely to be larger than 10% in the young plume (between 16% and 40% at 16 min, according to modeling studies by *Kärcher and Fahey* [1997], *Danilin et al.* [1997], and *Yu and Turco* [1997]). The modeling of heterogeneous processes between ambient species and particles within the plume and far wake is, we believe, unnecessary for prediction of the global impact of aircraft emissions because the amount of air processed within the wake is too small. Heterogeneous processing of aircraft-emitted species within the wake may prove to be important [*Kärcher,* 1997]. The impact of sulfur emissions from subsonic aircraft is not considered here (see *Friedl et al.,* [1997] for a discussion of possible tropospheric and climatic effects of subsonic sulfur emissions). However, future subsonic aircraft are expected to fly at higher altitudes, depositing a larger fraction of their emissions (including sulfur) in the stratosphere. These higher-flying subsonic aircraft should definitely be considered in modeling the impact of aviation on the future global environment.

Acknowledgments. Work at AER was supported by the NASA Atmospheric Effects of Aviation Program (AEAP) NAS1-19422 and the SAGE II program NAS1-20666. Novosibirsk State University acknowledges support from the Rus-

sian Foundation for Basic Research under grant 94-05-16661 and support from the U.S. National Aeronautics and Space Administration under grant NAG5-3409. We thank two anonymous reviewers for their helpful comments.

References

Albritton, D. L., et al., The atmospheric effects of stratospheric aircraft: Interim assessment report of the NASA high-speed research program, *NASA Ref. Publ. 1333,* 1993.

Asaturov, M. L., M. I. Budyko, K. Y. Winnikov, P. Y. Groysman, and A. S. Kabanov, *Volcanoes, Stratospheric Aerosols and the Climate of the Earth* (in Russian), 256 pp., Gidrometeoizdat, St. Petersburg, 1986.

Baughcum, S. L., and S. C. Henderson, Aircraft emission inventories projected in year 2015 for a high-speed civil transport (HSCT) universal airline network, *NASA Contractor Rep. CR-4659,* 1995.

Baughcum, S. L., et al., Stratospheric emissions effects database development, *NASA Contractor Rep. CR-4592,* 1994.

Bekki, S., and J. A. Pyle, Two-dimensional assessment of the impact of aircraft sulphur emission on the stratospheric sulphate aerosol layer, *J. Geophys. Res., 97,* 15,839-15,847, 1992.

Bekki, S., and J. A. Pyle, Potential impact of combined NO_x and SO_x emissions from future high speed civil transport aircraft on stratospheric aerosol and ozone, *Geophys. Res. Lett., 20,* 723-726, 1993.

Bekki, S., R. Toumi, J. A. Pyle, and A. E. Jones, Future aircraft and global ozone, *Nature, 354,* 193-194, 1991.

Borrmann, S., S. Solomon, J. E. Dye, D. Baumgardner, K. K. Kelly, and K. R. Chan, Heterogeneous reactions on stratospheric background aerosols, volcanic sulfuric acid droplets, and type I PSCs: Effects of temperature fluctuations and differences in particle phase, *J. Geophys. Res., 102,* 3639-3648, 1997.

Brasseur, G., M. H. Hitchman, S. Walters, M. Dymek, E. Falise, and M. Pirre, An interactive chemical dynamical radiative two-dimensional model of the middle atmosphere, *J. Geophys. Res., 95,* 5639-5655, 1990.

Brock, C. A., P. Hamill, J. C. Wilson, H. H. Jonsson, and K. R. Chan, Particle formation in the upper tropical troposphere: A source of nuclei for the stratospheric aerosol, *Science, 270,* 1650-1653, 1995.

Brown, R. C., R. C. Miake-Lye, M. R. Anderson, C. E. Kolb, and T. J. Resch, Aerosol dynamics in near-field aircraft plumes, *J. Geophys. Res., 101,* 22,939-22,953, 1996a.

Brown, R. C., M. R. Anderson, R. C. Miake-Lye, C. E. Kolb, A. A. Sorokin, and Y. Y. Buriko, Aircraft exhaust sulfur emissions, *Geophys. Res. Lett., 23,* 3603-3606, 1996b.

Brown, R. C., R. C. Miake-Lye, M. R. Anderson, and C. E. Kolb, Effect of aircraft exhaust sulfur emissions on near field plume aerosols, *Geophys. Res. Lett., 23,* 3607-3610, 1996c.

Chatfield, R. B., and P. J. Crutzen, Sulfur dioxide in remote oceanic air: Cloud transport of reactive precursors, *J. Geophys. Res., 89,* 7111-7132, 1984.

Chin, M., and D. D. Davis, A reanalysis of carbonyl sulfide as a source of stratospheric background sulfur aerosol, *J. Geophys. Res., 100,* 8993-9005, 1995.

Considine, D. B., A. R. Douglass, and C. H. Jackman, Effects of a polar stratospheric cloud parameterization on ozone depletion due to stratospheric aircraft in a two-dimensional model, *J. Geophys. Res., 99,* 18,879-18,894, 1994.

Danilin, M. Y., J. M. Rodriguez, M. K. W. Ko, D. K. Weisenstein, R. C. Brown, R. C. Miake-Lye, and M. R. Anderson, Aerosol particle evolution in an aircraft wake: Implications for the HSCT fleet impact on ozone, *J. Geophys. Res., 102,* 21,453-21,463, 1997.

DeMore, W. B., S. P. Sander, D. M. Golden, R. F. Hampson, M. J. Kurylo, C. J. Howard, A. R. Ravishankara, C. E. Kolb, and M. J. Molina, Chemical kinetics and photochemical data for use in stratospheric modeling, evaluation number 11, *JPL Publ. 94-26,* 1994.

Dyominov, I. G., The effect of the trace gas composition variations on the thermal regime of ozonosphere (in Russian), *Opt. Atmos., 1,* 63-72, 1988.

Dyominov, I. G., Investigations of spring anomaly of the total ozone in the Antarctic according to two-dimensional radiation-photochemical model (in Russian), *Atmospheric Ozone,* pp. 9-16, Leningrad Hydrometeorol. Instit., St. Petersburg, 1991.

Dyominov, I. G., On the photochemical mechanism of spring anomaly in stratospheric ozone over Antarctica (in Russian), *Investigations of the Atmospheric Ozone,* pp. 66-71, Gidrometeoizdat, Moscow, 1992.

Dyominov, I. G., and N. F. Elansky, The impact of supersonic aviation on the ozone layer: A chemical/microphysical model study, *Ann. Geophys., Part III, 13,* suppl. III, 700, 1995.

Dyominov, I. G., and A. M. Zadorozhny, The numerical simulation of anthropogenic impacts on the ozonosphere, *Atmospheric Ozone: Proceedings of the 1st American-Soviet Meeting on Atmospheric Ozone,* pp. 186-217, Gidrometeoizdat, Moscow, 1989.

Dyominov, I. G., and A. M. Zadorozhny, On the role of sulfate aerosols in estimation of the impact of supersonic aviation on the ozone layer, *Ann. Geophys., Part II, 14,* suppl. II, 507, 1996.

Dyominov, I. G., A. M. Zadorozhny, and N. F. Elansky, Global impact of Mount Pinatubo eruption on the composition and temperature of the ozonosphere, geophysics and the environment, paper presented at XXI General Assembly, Int. Union of Geod. and Geophys., Boulder, Colo., 1995.

Fahey, D. W., et al., Emission measurements of the Concorde supersonic aircraft in the lower stratosphere, *Science, 270,* 70-74, 1995.

Frenkel Y. I., *Kinetic Theory of Fluids* (in Russian), 592 pp., Nauka, St. Petersburg, 1975.

Friedl, R. R., et al., Atmospheric effects of subsonic aircraft: Interim assessment report of the advance subsonic technology program, *NASA Ref. Publ. 1400,* 1997.

Garcia, R. R., and S. Solomon, A numerical model of the zonally averaged dynamical and chemical structure of the middle atmosphere, *J. Geophys. Res., 88,* 1379-1400, 1983.

Ginzburg, E. I., and I. G. Dyominov, Numerical dynamical model of ozonosphere (in Russian), *Principles of Creating of Dynamic Model for Upper Atmosphere,* pp. 61-83, Gidrometeoizdat, Moscow, 1989.

Golitsyn, G. S. (Ed.), Study of the tropo/stratosphere gaseous composition changes and its influence on the climate and environment (in Russian), *Rep. 3,* Inst. for Atmos. Phys., Russ. Acad. of Sci., Moscow, 1994.

Hamill, P., R. P. Turco, C. S. Kiang, O. B. Toon, and R. C. Whitten, An analysis of various nucleation mechanisms for sulfate particles in the stratosphere, *J. Aerosol Sci., 13,* 561-585, 1982.

Hanson, D. R., and A. R. Ravishankara, Heterogeneous chemistry of bromine species in sulfuric acid under stratospheric conditions, *Geophys. Res. Lett., 22,* 385-388, 1995.

Hanson, D. R., A. R. Ravishankara, and S. Solomon, Heterogeneous reactions in sulfuric acid aerosols: A framework

for model calculations, *J. Geophys. Res., 99,* 3615-3629, 1994.

Hanson, D. R., A. R. Ravishankara, and E. R. Lovejoy, Reactions of $BrONO_2$ with H_2O on submicron sulfuric acid aerosol and the implications for the lower stratosphere, *J. Geophys. Res., 101,* 9063-9069, 1996.

Hitchman, M. H., and G. Brasseur, Rossby wave activity in a two-dimensional model: Closure for wave driving and meridional eddy diffusivity, *J. Geophys. Res., 93,* 9405-9417, 1988.

Hitchman, M. H., M. McKay, and C. R. Trepte, A climatology of stratospheric aerosol, *J. Geophys. Res., 99,* 20,689-20,700, 1994.

Hofmann, D. J., and J. M. Rosen, Balloon observations of a particle layer injected by a stratospheric aircraft at 23 km, *Geophys. Res. Lett., 5,* 511-514, 1978.

Johnston, H. S., D. E. Kinnison, and D. J. Wuebbles, Nitrogen oxides from high-altitude aircraft: An update of potential effects on ozone, *J. Geophys. Res., 94,* 16,351-16,363, 1989.

Kalnay, E., et al., The NCEP/NCAR 40-year reanalysis project, *Bull. Am. Meteorol. Soc., 77,* 437-471, 1996.

Kärcher, B., Heterogeneous chemistry in aircraft wakes: Constraints for uptake coefficients, *J. Geophys. Res., 102,* 19,119-19,135, 1997.

Kärcher, B., and D. W. Fahey, The role of sulfur emission in volatile particle formation in jet aircraft exhaust plumes, *Geophys. Res. Lett., 24,* 389-392, 1997.

Kent, G. S., and M. P. McCormick, SAGE and SAM II measurements of global stratospheric aerosol optical depth and mass loading, *J. Geophys. Res., 89,* 5303-5314, 1984.

Labitzke, K., J. J. Barnett, and B. Edwards (Eds.), *Middle Atmosphere Program, MAP Handbook,* v. 16, Univ. of Ill., Urbana, 1985.

Langner, J., and H. Rodhe, A global three-dimensional model of the tropospheric sulfur cycle, *J. Atmos. Chem, 13,* 225-263, 1991.

Larsen, N., Polar stratospheric cloud: A microphysical simulation model, *Dan. Meteorol. Inst. Sci. Rep., 91-2,* Copenhagen, 1991.

Michelsen, H. A., et al., Stratospheric ozone loss enhanced by aerosol reactions at temperatures above 200 K, paper presented at The 1997 Conference on the Atmospheric Effects of Aviation, Virginia Beach, Virginia, 1997.

Murphy, D. M., and A. R. Ravishankara, Temperature averages and rates of stratospheric reactions, *Geophys. Res. Lett., 21,* 2471-2474, 1994.

Pitari, G., Contribution to the ozone trend of heterogeneous reactions of $ClONO_2$ on the sulfate aerosol layer, *Geophys. Res. Lett., 20,* 2663-2666, 1993.

Pitari, G., S. Palermi, G. Visconti, and R. G. Prinn, Ozone response to a CO_2 doubling: Results from a stratospheric circulation model with heterogeneous chemistry, *J. Geophys. Res., 97,* 5953-5962, 1992.

Pitari, G., V. Rizi, L. Ricciardulli, and G. Visconti, High-speed civil transport impact: Role of sulfate, nitric acid trihydrate, and ice aerosols studied with a two-dimensional model including aerosol physics, *J. Geophys. Res., 98,* 23,141-23,164, 1993.

Plumb, R. A., A "tropical pipe" model of stratospheric transport, *J. Geophys. Res., 101,* 3957-3972, 1996.

Prather, M. J., and E. E. Remsberg (Eds.), The atmospheric effects of stratospheric aircraft: Report of the 1992 models and measurements workshop, *NASA Ref. Publ. 1292,* 1993.

Randeniya, L. K., P. F. Vohralik, I. C. Plumb, K. R. Ryan, and S. L. Baughcum, Impact of heterogeneous $BrONO_2$ hydrolysis on ozone trends and transient ozone loss during volcanic periods, *Geophys. Res. Lett., 23,* 1633-1636, 1996.

Stolarski, R. S., et al., 1995 scientific assessment of the atmospheric effects of stratospheric aircraft, *NASA Ref. Publ. 1381,* 1995.

Talrose V. L. (Ed.), Scientific basis for control of environment quality based on analysis of global bio-geochemical cycles for organogenic elements (in Russian), *Rep. 2,* Inst. of Energy Problems in Chem. Phys., Russ. Acad. Sci., Moscow, 1993.

Thomason, L. W., G. S. Kent, C. R. Trepte, and L. R. Poole, A comparison of the stratospheric aerosol background periods of 1979 and 1989-1991, *J. Geophys. Res., 102,* 3611-3616, 1997.

Tie, X. X., et al. The impact of high altitude aircraft on the ozone layer in the stratosphere, *J. Atmos. Chem., 18,* 103-128, 1994.

Toon, O. B., R. P. Turco, D. Westphal, R. Malone, and M. S. Liu, A multidimensional model for aerosols: Description of computational analogs, *J. Atmos. Sci., 45,* 2123-2143, 1988.

Turco, R. P., P. Hamill, O. B. Toon, R. C. Whitten, and C. S. Kiang, A one-dimensional model describing aerosol formation and evolution in the stratosphere, I, Physical processes and mathematical analogs, *J. Atmos. Sci., 36,* 699-717, 1979.

Weisenstein, D. K., M. K. W. Ko, J. M. Rodriguez, and N.-D. Sze, Impact of heterogeneous chemistry on model-calculated ozone change due to high speed civil transport aircraft, *Geophys. Res. Lett., 18,* 1991-1994, 1991.

Weisenstein, D. K., M. K. W. Ko, J. M. Rodriguez, and N.-D. Sze, Effects on stratospheric ozone from high-speed civil transport: Sensitivity to stratospheric aerosol loading, *J. Geophys. Res., 98,* 23,133-23,140, 1993.

Weisenstein, D. K., M. K. W. Ko, N.-D. Sze, and J. M. Rodriguez, Potential impact of SO_2 emissions from stratospheric aircraft on ozone., *Geophys. Res. Lett., 23,* 161-164, 1996.

Weisenstein, D. K., G. K. Yue, M. K. W. Ko, N.-D. Sze, J. M. Rodriguez, and C. J. Scott, A two-dimensional model of sulfur species and aerosols, *J. Geophys. Res., 102,* 13,019-13,035, 1997.

World Meteorological Organization (WMO), Scientific Assessment of Ozone Depletion: 1991, Global Ozone Res. and Monit. Proj., *Rep. 25,* Geneva, Switzerland, 1993.

WMO, Scientific Assessment of Ozone Depletion: 1994, Global Ozone Res. and Monit. Proj., *Rep. 37,* Geneva, Switzerland, 1995.

Yu, F., and R. P. Turco, The role of ions in the formation and evolution of particles in aircraft plumes, *Geophys. Res. Lett., 24,* 1927-1930, 1997.

Yue, G. K., L. R. Poole, P.-H. Wang, and E. W. Chiou, Stratospheric aerosol acidity, density, and refractive index deduced from SAGE II and NMC temperature data, *J. Geophys. Res., 99,* 3727-3738, 1994.

S. Bekki, Centre for Atmospheric Science, Department of Chemistry, University of Cambridge, Cambridge, England, U.K. (e-mail: slimane@atm.ch.cam.ac.uk)

I. Dyominov, Department for Atmospheric Research, Novosibirsk State University, Russia. (e-mail: dyominov@phys.nsu.nsk.su)

M. K. W. Ko and D. K. Weisenstein, AER, Inc., 840 Memorial Drive, Cambridge, MA 02139. (e-mail: mkwko @aer.com; dkweis@aer.com)

G. Pitari, L. Ricciardulli, and G. Visconti, Dipartimento di Fisica, Università degli Studi L'Aquila, Italy. (e-mail: pitari@aquila.infn.it; lucrezia@acd.ucar.edu; visconti@vxscaq.cineca.it)

(Received January 31, 1997; revised September 30, 1997; accepted September 30, 1997.)